Energy Engineering

Tech Science Press

https://doi.org/10.32604/ee.2026.078062

ARTICLE

Dual-Stage GT-RO-PCC Paradigm for Community-Integrated Energy Microgrid: Integrating Strategic Interaction and Uncertainty Mitigation

Siying Li[1], Xinyu Feng[2], Xin Ma[2], Hui Huang[2], Zhipeng Wang[2], Baolian Liu[2], Zujun Ding[2], Weihong Ding[2], Xiaolong Huang[2] and Jie Ji[2,*]

[1]School of Mechanical and Electrical Engineering, China University of Mining and Technology, Xuzhou, China
[2]Automation College, Huaian University, Huaiyin, China

*Corresponding Author: Jie Ji. Email: jijie@hyit.edu.cn

Received: 23 December 2025; Accepted: 19 January 2026; Published: 18 June 2026

ABSTRACT: This study introduces a novel Dual-Stage GT-RO-PCC (Game Theory-Robust Optimization-Price Coupling Control) paradigm to address operational challenges in community-integrated energy microgrids (CIEMs) characterized by multi-energy complementarity and distributed generation. By synergizing strategic interaction mechanisms with uncertainty-aware energy management, the proposed framework establishes a tripartite governance structure integrating microgrid operators, user-side aggregators, and shared energy storage operators. The first stage formulates a Stackelberg game-theoretic model to optimize day-ahead electricity/heat pricing strategies through bilevel optimization, incorporating flexible load management modeling with flexible load disaggregation and carbon emission trading mechanisms. The second stage constructs a two-stage stochastic robust optimization model addressing Weibull-distributed wind power uncertainty and demand prediction errors under 3σ confidence intervals, ensuring supply reliability while minimizing operational costs. Empirical validation on a representative community microgrid demonstrates superior performance: daily operational cost reduction of ¥4965.00 (−13.2% vs. baseline), wind/PV accommodation rates of 98.76%/98.91%, peak energy storage arbitrage revenue of ¥658.20/day, 96.95% carbon reduction (1673 kg CO/day) via power-carbon synergy, and 98.6% supply resilience under Monte Carlo-simulated extreme scenarios. Theoretical contributions include a GT-RO-PCC framework integrating non-cooperative game theory with distributionally robust optimization, a hierarchical decision protocol for asymmetric multi-entity CIEMs, and a bi-level uncertainty quantification methodology for low-carbon distribution network planning. This paradigm advances uncertainty-robust energy management, offering systematic solutions for high-renewable penetration in Community-integrated Energy Microgrid and supporting China's dual-carbon objectives.

KEYWORDS: GT-RO-PCC paradigm; two-stage optimization; strategic interaction mechanism; uncertainty-aware energy management; power-carbon synergy; distributed renewable integration

1 Introduction

The global energy paradigm is undergoing a profound transformation, driven by escalating energy demand and the accelerated integration of renewable energy sources into power systems [1]. Community-integrated energy microgrids (CIEMs), characterized by multi-energy complementarity and distributed generation paradigms, have emerged as a promising paradigm to enhance energy efficiency and resilience. However, their operational complexity is amplified by dual pressures: the intermittency/volatility of renewable resources (e.g., wind/solar) and the stochasticity of load demands. These uncertainties pose significant challenges for source-load coordination, particularly within thermal-electric coupling frameworks where

traditional scheduling paradigms exhibit systemic inefficiencies [2]. While existing literature has explored distributed energy resource management, critical gaps persist in three domains: (1) modeling synergies between thermal-cooling subsystems, (2) developing adaptive mechanisms for external market dynamics, and (3) formulating scalable economic frameworks that reconcile operational costs with equitable benefit distribution. Moreover, conventional game-theoretic approaches for intra-microgrid resource allocation often fail to integrate robust optimization techniques, leading to excessive conservatism in uncertain environments. To bridge these gaps, this study introduces a Dual-Stage GT-RO-PCC (Game Theory-Robust Optimization-Price Coupling Control) paradigm, synergizing non-cooperative game theory with distributionally robust optimization to establish a tripartite governance structure among microgrid operators, user aggregators, and shared energy storage providers. This tripartite design is critical for decentralizing decision-making in CIEMs, where asymmetric information and conflicting objectives exist. The microgrid operator acts as a profit-maximizing leader, user aggregators adjust loads based on price signals, and storage providers enable temporal arbitrage—each entity's strategies are interdependent, necessitating a game-theoretic equilibrium. Lack of integrated PCC mechanisms, limited multi-entity coordination. The proposed framework advances two-stage decision-making: (i) a Stackelberg game-theoretic model optimizes day-ahead electricity/heat pricing through bilevel optimization, incorporating flexible load disaggregation and carbon emission trading mechanisms; (ii) a two-stage stochastic robust optimization model addresses Weibull-distributed wind power uncertainty and load forecasting errors under 3σ confidence intervals, ensuring supply reliability while minimizing lifecycle costs. Empirical validation on a representative CIEM demonstrates superior performance, achieving a 13.2% reduction in daily operational costs (¥4965.00 vs. baseline), 98.76%/98.91% wind/PV accommodation rates, and 96.95% carbon reduction (1673 kg CO_2/day) via electricity-carbon coupling. Theoretical contributions include: (a) a GT-RO-PCC framework that explicitly couplesday-ahead pricing with real-time uncertainty mitigation via a bilevel feedback loop; (b) a hierarchical protocol that reduces operational costs by 13.2% under uncertainty, outperforming baseline methods; (c) a distributionally robust model that achieves 98.6% supply resilience, exceeding typical stochastic programming approaches. Unlike existing frameworks that treat pricing and uncertainty management as sequential processes, our GT-RO-PCC paradigm introduces a feedback-driven Price Coupling Controlloop, where day-ahead Stackelberg game outcomes directly inform robust optimization constraints, ensuring adaptive resilience to market and supply-demand fluctuations. This work advances the frontier of uncertainty-robust energy management, offering actionable solutions for high-renewable penetration in community microgrids and supporting China's dual-carbon objectives through power-carbon synergy and distributed renewable integration.

Significant advancements have been achieved in community-integrated energy microgrid (CIEM) research. However, AI-based approaches often overlook multi-stakeholder strategic interactions, while game-theoretic models fail to leverage distributionally robust learning for uncertainty quantification. Our work bridges this gap by hybridizing AI-enhanced forecasting with non-cooperative game theory. Reliability-conscious power flow optimization in hybrid renewable microgrids: a case study in Sub-Saharan Africa using Gauss-Seidel and metaheuristic techniques [2]. With seminal works delineating key paradigms and technical frontiers. Literature [3] provides a comprehensive analysis of zero-carbon microgrids, highlighting their pivotal role in energy decarbonization while elucidating technical challenges and prospective solutions. Literature [4] advances the field by proposing innovative design and monitoring frameworks for sustainable green energy networks, emphasizing microgrid-enabled improvements in energy efficiency and system reliability. In parallel, Literature [5] introduces an intelligent demand forecasting and energy management model, leveraging advanced analytics to optimize allocation and mitigate waste in renewable-dominated systems. Notwithstanding these strides, Literature [6] underscores the economic and technical hurdles in

deploying hydrogen-based zero-carbon microgrids in remote regions, despite demonstrating their feasibility as resilient energy solutions. Further, Literature [7] advances techno-economic methodologies for isolated microgrids with high renewable penetration, yet falls short in addressing multi-energy synergies and distributed governance mechanisms. Collectively, these studies establish foundational frameworks but overlook critical synergies between thermal-cooling subsystems, adaptive market-responsive mechanisms, and cross-disciplinary uncertainty quantification. To bridge these gaps, this study pioneers a Dual-Stage GT-RO-PCC (Game Theory-Robust Optimization-Price Coupling Control) paradigm, synergizing strategic interaction modeling with distributionally robust optimization to establish a tripartite governance structure among microgrid operators, user aggregators, and shared energy storage providers.

Community-integrated energy microgrids (CIEMs) have emerged as a promising paradigm to enhance energy efficiency and resilience. However, their operational complexity is amplified by the intermittency of renewables and load stochasticity. While existing studies [8] address distributed energy management, critical gaps persist in modeling thermal-cooling synergies, adaptive market mechanisms, and scalable economic frameworks. Recent AI-based approaches [9] focus on data-driven forecasting but overlook multi-entity strategic interactions, whereas game-theoretic models [10] lack integration with distributionally robust optimization.

To bridge these gaps, this study introduces a Dual-Stage GT-RO-PCC paradigm, synergizing non-cooperative game theory with distributionally robust optimization. The framework establishes a tripartite governance structure among microgrid operators, user aggregators, and storage providers, where the Price Coupling Control (PCC) mechanism dynamically couples day-ahead Stackelberg game outcomes with real-time uncertainty mitigation.

Theoretical contributions include: (a) a GT-RO-PCC framework that reduces operational costs by 13.2% under uncertainty; (b) a hierarchical protocol ensuring 98.6% supply resilience; (c) a bi-level uncertainty quantification methodology tailored for low-carbon distribution networks.

Despite significant advancements in microgrid technology, numerous challenges persist in their widespread implementation and operation. Microgrids, which integrate multiple distributed energy resources (DERs) and complex control equipment, require effective management mechanisms and robust communication channels to ensure coordinated operation and scheduling. These measures are essential for maintaining the overall stability and reliability of the power system. The evolving societal demands for energy further complicate the situation. In addition to the need for a stable electricity supply, there is a growing demand for heat and cooling services. However, existing microgrid technologies often fall short in meeting these multifaceted energy demands, and research addressing this gap remains limited. Moreover, economic barriers pose significant hurdles to the large-scale deployment of microgrids. Power electronic equipment suitable for microgrids is typically expensive, and the long payback periods associated with distributed power generation devices diminish their operational economic viability. These factors collectively restrict the widespread adoption and commercialization of microgrids. To address these challenges, particularly the issue of equitable benefit distribution among microgrid stakeholders, it is imperative to introduce game-theoretic models. By leveraging the distribution mechanisms inherent in cooperative game theory, the economic benefits derived from microgrid operations can be allocated fairly and efficiently. This approach not only enhances the enthusiasm of various participants in the construction and operation of microgrids but also fosters greater engagement and motivation. Specifically, game theory can be employed to design flexible load management mechanisms. For instance, an incentive-based flexible load management game can be implemented, wherein power suppliers act as one player, offering various incentives such as electricity price subsidies or priority power supply. Users, as the counterpart, can then adjust their electricity consumption strategies based on these incentives and their individual needs. This mechanism ensures user satisfaction

while achieving effective load management, thereby improving the reliability and economic efficiency of microgrids.

The integration of game theory into microgrid management has garnered significant attention, with several studies demonstrating its potential for optimizing energy resource allocation and enhancing operational efficiency. For instance, Literature [11] employs Nash bargaining theory to optimize multi-microgrid electricity sharing operations. By considering factors such as multi-energy coordination and carbon emissions, this study establishes models and solution methods that maximize the benefits of microgrid alliances and ensure fair distribution of cooperative gains. Literature [12] focuses on the unique challenges of islanded microgrids, utilizing game theory to address the coordinated optimization of distributed energy resources. This research highlights the potential for improving the self-sufficiency and stability of islanded microgrids through strategic resource management. Literature [13] introduces a hierarchical game-theoretic approach that accounts for the layered structure and diverse interests of entities within microgrids. This method aligns more closely with real-world operational and management scenarios, effectively resolving conflicts and interest discrepancies among stakeholders while enhancing the efficiency and flexibility of energy management. Literature [14] investigates peer-to-peer energy trading in microgrids through game theory analysis, exploring the application of various game models. This study underscores the potential for fostering competitive and cooperative relationships among distributed energy resources and energy storage devices, therebyboosting the market competitiveness of microgrids. Literature [15] adopts a risk-averse game-theoretic framework to study investment and operational decision-making in microgrids. By considering uncertainties and risk factors inherent in microgrid operations, this research provides valuable insights into resilient and adaptive management strategies. Collectively, these studies demonstrate that game theory can optimize energy resource allocation within microgrids. Through strategic interactions among distributed energy resources and energy storage devices, microgrids can establish competitive and cooperative dynamics, enhancing overall market performance. In the context of electricity markets, microgrid operators integrate multiple cost considerations, load forecasts, and other factors to engage in strategic games with other large power generation enterprises or microgrids, aiming to maximize benefits. However, the practical operation of microgrids presents complexities and variabilities that challenge the effectiveness of these optimization strategies. Distributed energy output is dynamically influenced by factors such as weather conditions, which often deviate from the assumptions made in theoretical models. This discrepancy can lead to suboptimal performance when applying these strategies in real-world scenarios. Moreover, existing models predominantly focus on internal game-theoretic relationships within microgrids, neglecting external interference factors such as sudden policy changes and natural disasters. Technical and systemic integration issues also arise when incorporating game theory into microgrid operations. The integration of game-theoretic approaches with other essential technologies—such as distributed energy control and energy storage management—remains underdeveloped. Compatibility problems may emerge during system integration, as resource allocation schemes derived from game theory may not be effectively implemented within existing microgrid hardware and software systems. This incompatibility necessitates extensive modifications and upgrades, thereby increasing application costs and implementation difficulties.

Due to the existence of multiple uncertain factors in microgrids, such as the intermittent power generation of renewable energy (solar energy, wind energy, etc.), the uncertainty of load demand, significant differences in user demands in different time periods, and uncertainties caused by power transmission. Therefore, the introduction of robust optimization is a crucial aspect in the development of microgrids. Robust optimization can take into account the uncertainties of renewable energy generation and load demand to determine the optimal energy storage charging and discharging strategies. Meanwhile, robust optimization can also consider the costs and benefits of different energy resources. Under uncertain

conditions, it can reasonably select the input and use sequence of energy resources. For example, considering the price fluctuations of natural gas and the uncertainty of solar power generation, robust optimization can be used to determine when to use natural gas for power generation and when to rely on solar power generation, so as to achieve the optimal balance between operational economic benefits and energy utilization efficiency. Literature [16] proposes a short-term operation model based on the min-max-min robust framework for microgrids containing natural gas networks to capture the uncertainties of wind power generation and electrical/thermal loads. Literature [17] takes into account the impact of the uncertainties of renewable energy and the time-coupling constraints of energy storage systems on the operational feasibility of regional microgrids and proposes a multi-stage power generation scheduling method for regional microgrids to ensure the robustness and non-anticipativity of the scheduling scheme simultaneously. Literature [18] takes the synchronization between microgrids and utilities as the research background, regards the uncertainties of the microgrid dynamic model as multiplicative perturbations, and designs a robust controller based on the robust control principle through μ-synthesis analysis to improve the robust stability and performance of the system. Literature [19] proposes a data-driven robust optimization method to solve the microgrid scheduling problem under the uncertainty of wind power generation. By collecting a large amount of historical wind speed data, it uses machine learning algorithms to predict the probability distribution of wind power generation and constructs a robust optimization model on this basis. Literature [20] distinguishes the typical operation modes of microgrids by using the k-means++ algorithm and generalizes the equivalent model parameters by using a convolutional neural network, realizing the robust simplified modeling of microgrids under different typical operation modes. This method can accurately reflect the real response of the system under unknown faults. Therefore, the introduction of robust optimization for microgrids can effectively cope with the uncertainty of loads, enhance the stability of the system, and improve the reliability of decision-making [21]. However, robust optimization models consider the worst-case scenarios in order to deal with uncertainties, which may lead to overly conservative models. In microgrids, such models may overestimate uncertain factors such as the fluctuations of distributed energy and load changes, resulting in relatively low resource allocation efficiency of the obtained optimization schemes. Meanwhile, there are also difficulties in integrating robust optimization with other existing control and management strategies in microgrids [22]. There are already multiple mature control methods in microgrids, such as the maximum power point tracking control of distributed power sources and the charging and discharging control of energy storage devices. After introducing robust optimization, how to effectively combine it with these existing strategies and make it play the advantages of robust optimization without affecting the performance of the original system is a problem that needs to be solved [23]. In the current research field, the robustness of microgrids has been significantly enhanced. However, relatively little research has been conducted on multi-energy systems.

Existing research on the optimal operation of community-based microgrids has identified deficiencies in the coordinated management of multiple distributed energy resources (DERs) and the response to complex external environmental changes [24]. These challenges are further compounded when considering the intertwined influences of the interest demands of different entities and uncertainty factors, highlighting the lack of a comprehensive theoretical and methodological framework [23]. To address these gaps, this study proposes an integrated approach that combines game theory with robust optimization for community-based microgrids. These microgrids typically consist of multiple distributed energy generation units (e.g., solar and wind energy), energy storage devices, and numerous electricity users. The proposed approach leverages game theory to establish strategic interaction models among these entities, clarifying decision-making mechanisms in energy trading and power allocation. This enables efficient resource allocation and balances the interests of all parties. Additionally, robust optimization is employed to handle external

interference factors such as the intermittency of renewable energy generation, load demand uncertainty, and potential equipment failures, thereby ensuring stable microgrid operation under adverse conditions. This comprehensive approach effectively resolves several operational issues in community-based microgrids, including inefficient resource allocation, difficulty in coordinating interests among stakeholders, and poor system stability and reliability in the face of uncertainties. It enhances energy utilization efficiency, promotes the benign interaction and development of the community energy market, and lays a solid foundation for the extensive application and sustainable development of community-based microgrids. The core contributions of this study are fourfold. First, a game-theoretic source-load optimization scheduling model is proposed, enabling microgrid operators and user-side aggregators to dynamically adjust their electricity and heat purchases based on each other's strategies. This model optimizes pricing strategies, reduces daily operational costs to 5721 yuan, and increases the consumption rates of wind and photovoltaic energy to 89.67% and 91.98%, respectively. Second, a two-stage robust optimization model is constructed to minimize operational costs under uncertainty, achieving a minimum daily cost of 4965 yuan, energy storage revenue of 658.2 yuan, and consumption rates of wind and photovoltaic energy reaching 98.76% and 98.91%, respectively. Third, a power-carbon synergy mechanism is introduced to promote renewable energy consumption and low-carbon development, reducing carbon emissions by 96.95% compared to baseline scenarios. Finally, the study provides theoretical guidance and practical solutions for stable power system operation, maximization of operational economic benefits, and renewable energy integration. The robustness of the model against disturbances is verified through Monte Carlo simulations, demonstrating good performance under adverse scenarios. These contributions hold significant value for both theoretical advancements and practical applications in the field of community-based microgrid management.

In this study, we propose an innovative source-load optimization scheduling framework that integrates game theory with two-stage robust optimization, specifically tailored to address the operational challenges in community integrated energy microgrids (CIEMs). The primary objectives of this framework are to minimize operational costs and enhance system robustness, thereby ensuring reliable and economically efficient energy management within CIEMs.

To achieve these goals, we first establish a comprehensive integrated energy microgrid framework that incorporates multiple stakeholders, including microgrid operators, user-side aggregators, and shared energy storage operators. This framework enables a detailed analysis of the operational strategies and interdependencies among these entities, facilitating a holistic understanding of the system dynamics.

Building on this foundation, we introduce a one-stage game strategy to facilitate interactive optimization between microgrid operators and user-side aggregators. This strategic interaction allows for dynamic adjustments in pricing and load management, thereby improving overall system efficiency and economic viability. Concurrently, we construct a two-stage stochastic robust optimization model that explicitly considers uncertainties in renewable energy generation and load demands. By incorporating these uncertainties, the model effectively minimizes operational costs while ensuring system stability and reliability under varying conditions.

Through extensive case studies and analyses, we demonstrate the validity and superiority of the proposed model. The results provide robust theoretical support and practical insights for the stable operation of power systems, the maximization of operational economic benefits, and the effective integration of renewable energy sources. This research thus offers a systematic solution to enhance the performance and sustainability of community integrated energy microgrids.

Compared to standalone game-theoretic models or robust optimization, GT-RO-PCC uniquely integrates strategic interaction with uncertainty-aware control, enabling dynamic pricing and carbon synergy.

2 Methodology

2.1 Framework of the Integrated Energy Microgrid

The community integrated energy microgrid is conceptualized as a system comprising three key entities: microgrid operators, user-side aggregators, and shared energy storage operators. This tripartite structure forms the basis for the subsequent analysis and modeling. For a detailed visualization of this framework, please refer to Fig. 1.

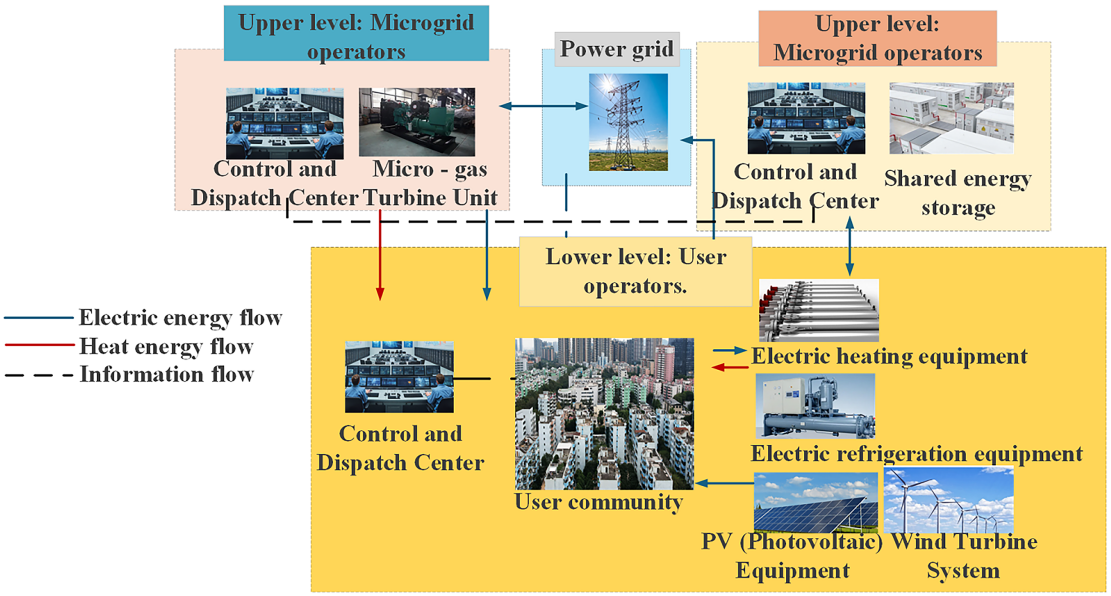

Figure 1: Framework of the community integrated energy microgrid.

The Price Coupling Control (PCC) mechanism operates as a dynamic feedback loop between the two optimization stages. As shown in Fig. 2, PCC continuously adjusts day-ahead pricing strategies based on real-time robust optimization outcomes through the constraint:

$$\lambda_h^{\mathrm{MGO}_s}(k+1) = \lambda_h^{\mathrm{MGO}_s}(k) + \alpha \cdot \frac{\partial C_{\mathrm{robust}}}{\partial \lambda_h^{\mathrm{MGO}_s}}$$

where $\lambda_h^{\mathrm{MGO}_s}$ is the adaptation gain and k denotes the iteration index. This closed-loop control ensures adaptive response to uncertainty realizations.

The microgrid operator functions as an intermediary between the power grid and end-users, facilitating energy transactions on the user side. From a market perspective, the operator sets rational pricing for electricity and heat, enabling energy trading with users and thereby generating profits. Physically, the operator is equipped with essential facilities such as gas turbines, which allow the provision of both electrical and thermal energy services to users.

The shared energy storage operator is assumed to primarily provide energy storage services for user-side aggregators, enhancing the flexibility of load adjustments on the user side. This operator charges service fees based on the capacity stored or withdrawn by users, with the unit capacity rental fee influencing users' willingness to utilize these services.

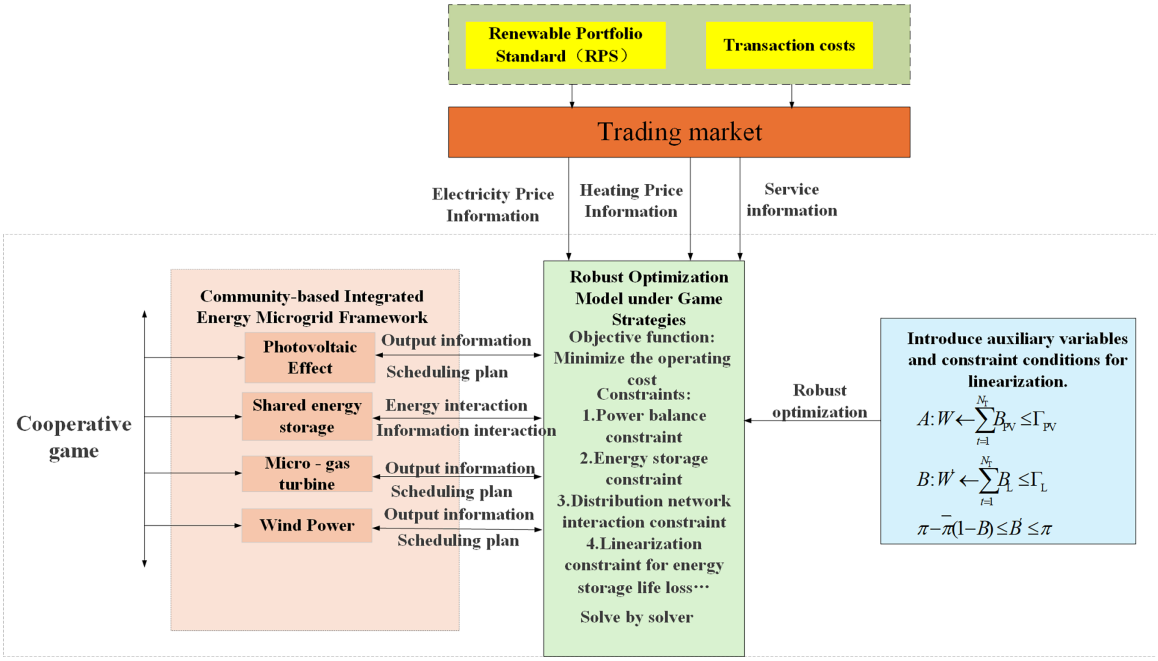

Figure 2: Two-stage robust smart source-load optimization block diagram based on game theory.

The user-side load comprises both electrical and thermal loads, with each user equipped with photovoltaic (PV) installations. Additionally, the system includes wind power generation devices. Given that the electricity selling price set by the microgrid operator is lower than that of the grid, users are assumed to purchase electricity exclusively from the microgrid operator and sell excess electricity to the grid. When user-side PV generation is insufficient to meet electrical loads, users can either purchase electricity from the microgrid operator or draw energy from the shared energy storage system. Conversely, surplus PV power can be sold to the grid or stored in the shared energy storage system. For thermal loads, a portion is supplied by micro gas turbines operated by the microgrid operator, while the remainder is provided by electric heating equipment on the user side. This dual-source structure for electrical and thermal energy increases the flexibility of the user-side energy supply.

The operational modes of each entity within the microgrid are as follows: The microgrid operator establishes electricity purchase and selling prices in advance, based on the time-of-use electricity prices of the grid for the following day. In response, user-side aggregators optimize the distribution of electrical and thermal loads within a day, considering the electricity prices set by the microgrid operator and the rental fees charged by the energy storage supplier. Users can further enhance their benefits by leveraging shared energy storage services.

2.1.1 Microgrid Operator Model

Let $\lambda_h^{\mathrm{EG},b}$, $\lambda_h^{\mathrm{MGO},s}$, $\lambda_h^{\mathrm{EG},s}$ denote grid purchase price, MGO sale price, and grid sale price in period h, with constraints:

$$\lambda_h^{\mathrm{EG},b} + \delta \le \lambda_h^{\mathrm{MGO},s} \le \lambda_h^{\mathrm{EG},s} - \delta \tag{1}$$

$$\gamma_h^{\min} \le \gamma_h^{\mathrm{MGO},s} \le \gamma_h^{\max} \tag{2}$$

where δ = ¥0.05/kWh ensures arbitrage viability, and heat price bounds derive from production costs:

$$\gamma_h^{\min} = \frac{C_{mv}}{\eta_h}, \quad \gamma_h^{\max} = \gamma^{\mathrm{NG}} \times (1 + \mathrm{margin}\%) .$$

The micro-gas turbine provides electricity and heat energy for the user side. The relationship between its fuel cost and the output electric power of the unit group in$h$time periods within a day can be expressed as:

$$R_h^{\mathrm{MT}} = \frac{Z_{ng}}{Z\eta_{\mathrm{e}}^{\mathrm{MT}}} W_h^{\mathrm{MT,e}} \tag{3}$$

In the formula, $W_h^{\mathrm{MT,e}}$ is the electric power output by the micro-gas turbine in the h-th time period within a day, Z_{ng} is the unit price of the fuel, Z is the heat value of the fuel, and $\eta_{\mathrm{e}}^{\mathrm{MT}}$ is the power generation efficiency of the micro-combustion unit group.

The relationship between electricity and heat output of the micro-gas turbine in the h-th time period can be expressed as:

$$R_h^{\mathrm{MT,h}} = \frac{1 - \eta_{\mathrm{e}}^{\mathrm{MT}} - \eta_{\mathrm{loss}}^{\mathrm{MT}}}{\eta_{\mathrm{e}}^{\mathrm{MT}} Q} \eta_{\mathrm{B}} P_h^{\mathrm{MT,e}} Z \tag{4}$$

In the formula, $R_h^{\mathrm{MT,h}}$ is the heat power output by the gas turbine in the h-th time period, $\eta_{\mathrm{loss}}^{\mathrm{MT}}$ is the metal heat dissipation loss rate, Q is the concentration of nitrogen oxides, η_{B} is the heating coefficient, and Z is the heat value of the fuel.

Considering the supply-demand balance relationship of heat power, there is:

$$R_h^{\mathrm{MT,h}} = J_h^{\mathrm{MGO,h}} \tag{5}$$

In the formula, $J_h^{\mathrm{MGO,h}}$ represents the thermal power purchased by the user aggregator from the microgrid operator in the h-th time period of the day.

For wind power generation systems, v_{in}, v_r and v_{out} are used to represent the cut-in wind speed, rated wind speed, and cut-out wind speed of the wind power generation system, respectively. When the wind speed is lower than v_{in} or higher than v_{out}, the wind power generation system stops generating electricity. When the wind speed is within the range of v_{in} and v_r, the power generation efficiency of the wind power generation system gradually increases with the increase of wind speed. When the wind speed is within the range of v_r and v_{out}, the wind turbine operates at the rated power. However, due to the uncertainty, volatility, and intermittency of wind speed, assuming that the wind speed follows the Weibull [25] distribution, the formula of the wind power generation system is:

$$E_W(t) = \begin{cases} 0, 0 \le v(t) \langle v_{in}, v(t) \rangle v_{out} \\ 0.5\pi r^2 \rho v(t)^3, v_{in} \le v(t) < v_r \\ P_W^r, v_r \le v(t) \le v_{out} \end{cases} \tag{6}$$

Among them, r is the radius of the circle formed when the blade rotates, ρ is the air density, and P_W^r is the rated power of the wind power generation system.

The Weibull expression formula is:

$$f(v) = \begin{cases} \alpha v^{\alpha-1} e^{-v^{\alpha}}, & \alpha > 0; \\ 0, & \text{other.} \end{cases} \tag{7}$$

α is the shape parameter of the Weibull distribution, which can be obtained based on wind speed historical data.

Among them, the income of the micro-grid operator within a day can be expressed as:

$$E_{\mathrm{MGO}} = E_{\mathrm{MGO}}^{\mathrm{EG,e}} + E_{\mathrm{MGO}}^{l,e} + E_{\mathrm{MGO}}^{l,\mathrm{h}} - C_{\mathrm{MT}} - C_{\mathrm{WIND}} \tag{8}$$

$E_{\mathrm{MGO}}^{\mathrm{EG,e}}$,$E_{\mathrm{MGO}}^{l,e}$, and $E_{\mathrm{MGO}}^{l,\mathrm{h}}$ respectively represent the income of the micro-grid operator's daily transactions with the power grid, the user-side power transactions, and the income generated by heating for the user-side. C_{MT} represents the gas cost of the micro-grid operator for a day, and C_{WIND} represents the cost of the micro-grid operator's wind power generation system for a day. The formula can be further expressed as:

$$E_{\mathrm{MGO}}^{\mathrm{EG,e}} = \sum_{h=1}^{H} \frac{-\lambda_h^{\mathrm{EG,s}} \cdot \max\left(q_h^{l,\mathrm{c}} - W_h^{\mathrm{MT,e}}, 0\right)}{-\lambda_h^{\mathrm{EG,b}} \cdot \min\left(q_h^{l,\mathrm{c}} - W_h^{\mathrm{MT,e}}, 0\right)} \tag{9}$$

$$E_{\mathrm{MGO}}^{l,\mathrm{e}} = \lambda_h^{\mathrm{MGO,s}} \max\left(L_h^{l,\mathrm{c}}, 0\right) \tag{10}$$

$$E_{\mathrm{MGO}}^{l,\mathrm{h}} = \sum_{h=1}^{H} \left(u_h L_h^{\mathrm{MGO,h}} \gamma_h^{\mathrm{MGO,s}}\right) \tag{11}$$

$$C_{\mathrm{MT}} = \sum_{h=1}^{H} C_{\mathrm{MT,h}} \tag{12}$$

$$C_{\mathrm{WIND}} = \sum_{h=1}^{H} C_{\mathrm{WIND,h}} \tag{13}$$

In the formula, $q_h^{l,\mathrm{c}}$ is the net electrical load of the user aggregator within the h-th time period during the day.

2.1.2 The Model of Shared Energy—Storage Service Providers

The shared energy storage system is set as an independent system and independently configured on the side of the shared energy storage operator, aiming at the storage and utilization of electricity for the community's electricity. Consider a community-type integrated energy micro-grid with n users. Assume that a day can be divided into H time periods. The capacity of the shared energy storage system at the $h+1$-th moment can be expressed as:

$$E_{h+1}^{\mathrm{ESS}} = E_h^{\mathrm{ESS}} + \left(\eta_{\mathrm{c}}^{\mathrm{ESS}} P_h^{I,\mathrm{c}} - \frac{P_h^{I,\mathrm{d}}}{\eta_{\mathrm{d}}^{\mathrm{ESS}}}\right) \Delta t \tag{14}$$

In the formula, $P_h^{I,c}$ and $P_h^{I,d}$ represent the charging and discharging power of the user aggregator in the community within the h-th time period, respectively; η_c^{ESS} and η_d^{ESS} represent the transmission efficiencies of users in the charging and discharging processes, respectively; Δt is the time interval from the moment h to the next moment $h+1$.

The net energy change over H periods must be zero for cyclic operation:

$$\sum_{h=1}^{H}\left(\eta_h^{ESS}p_h^{l,c}-\frac{p_h^{l,d}}{\eta_d^{ESS}}\right)\Delta t=0 \tag{15}$$

with complementary constrain $p_h^{l,c}\cdot p_h^{l,d}=0\forall h$, to prevent simultaneous charge/discharge, that is, the system capacity constraint conditions are met:

$$E_{min}^{ESS}\le E_h^{ESS}\le E_{max}^{ESS} \tag{16}$$

E_{min}^{ESS} and E_{max}^{ESS} are the minimum and maximum values of the shared energy storage system capacity.

And possibly within the time period h, due to the charging and discharging power being subject to the allowable power limit of the shared energy storage system, the following constraint conditions exist:

$$\begin{cases}\left|\frac{E_{h+1}^{ESS}-E_h^{ESS}}{\Delta t}\right|\le P_{max}^{ESS,c}\left(P_h^{l,c}\le P_h^{l,d}\right)\\ \left|\frac{E_{h+1}^{ESS}-E_h^{ESS}}{\Delta t}\right|\le P_{max}^{ESS,d}\left(P_h^{l,c}\ge P_h^{l,d}\right)\end{cases} \tag{17}$$

In the formula, $P_{max}^{ESS,c}$ and $P_{max}^{ESS,d}$ are the maximum charging power and discharging power allowed by the shared energy storage system, respectively.

When users use the shared energy storage system, they need to pay corresponding service fees. The total cost that users need to pay on the user side within a day can be expressed as:

$$C_+^{ESS}=\sum_{h=1}^{H}\lambda_h^{ESS}\left(P_h^{l,c}+P_h^{l,d}\right) \tag{18}$$

In the formula, λ_h^{ESS} represents the lease fee that needs to be paid to the energy storage service provider for unit charging power or unit discharging power in the h-th time period.

At the same time, the charging and discharging cost expenses that the shared energy storage service provider needs to pay are expressed as:

$$C_-^{ESS}=\sum_{h=1}^{H}\left(\lambda_c P_h^{l,c}\Delta t+\lambda_d P_h^{l,d}\Delta t\right) \tag{19}$$

λ_c and λ_d are the unit charging and discharging cost coefficients of the shared energy storage system, respectively.

In summary, the revenue function of the shared energy storage service provider within a day can be expressed as:

$$C^{ESS}=C_+^{ESS}-C_-^{ESS} \tag{20}$$

2.1.3 User-Side Flexible Load and Energy Storage Integration Model

Considering the user-side load characteristics, electrical loads are categorized into rigid and flexible electrical loads. Rigid electrical loads exhibit limited flexibility and can only receive power supply during fixed time periods, whereas flexible electrical loads possess higher flexibility and do not require a fixed power supply schedule. This distinction allows for more effective load management strategies, such as load shifting, which can optimize the overall energy balance within the microgrid.

$$Q_h^{l,\mathrm{e}} = Q_h^{l,\mathrm{f}} + Q_h^{l,\mathrm{s}} + \Delta Q_h^{l,\mathrm{e}} \tag{21}$$

$Q_h^{l,\mathrm{e}}$, $Q_h^{l,\mathrm{f}}$,$Q_h^{l,\mathrm{s}}$ and $\Delta Q_h^{l,\mathrm{e}}$ respectively represent the total electrical load, rigid electrical load, flexible electrical load, and electrical load consumed by electric heating of the user aggregator within a day.

In order to uniformly describe the demand-response capability on the user side, we automatically need the flexible electrical loads of all users. The demand-response capability is measured by the proportion ε that can be adjusted in each time period and the total proportion k of the electricity quantity adjustment. Meanwhile, the following constraints are set for the flexible electrical load adjustment of the user aggregator:

$$\frac{\left|\overline{Q_h^{l,s}} - Q_h^{l,s}\right|}{Q_h^{l,f} + Q_h^{l,s}} \le N \tag{22}$$

$$\sum_{h=1}^{H}\left|\overline{Q_h^{l,\mathrm{s}}} - Q_h^{l,\mathrm{s}}\right| = k\sum_{h=1}^{H}\left(Q_h^{l,\mathrm{f}} + Q_h^{l,\mathrm{s}}\right) \tag{23}$$

$$\sum_{h=1}^{H}\overline{Q_h^{l,\mathrm{s}}} = \sum_{h=1}^{H} Q_h^{l,\mathrm{s}} \tag{24}$$

$\left|\overline{Q_h^{l,s}} - Q_h^{l,s}\right|$ represents the electrical load adjustment amount of the user in the h-th time period within a day without considering $\Delta Q_h^{l,\mathrm{e}}$. $\overline{Q_h^{l,\mathrm{s}}}$ represents the flexible electrical load of the user aggregator adjusted in the h-th time period within a day. N represents the maximum allowable proportion of the electrical load adjustment amount in the h-th time period within a day. k represents the proportion of the total electrical load adjustment amount of the user aggregator within a day. The larger N and k are, the more flexible the load adjustment performance in the time period is, and the greater the demand-response capability of the user side is.

The user side can store and retrieve electrical energy at any time period. Considering the response demand of the user-side electrical load comprehensively, the net electrical load of the user in the h-th time period within a day is:

$$Q_h^{l,\mathrm{c}} = Q_h^{l,\mathrm{f}} + \overline{Q_h^{l,\mathrm{s}}} + \Delta Q_h^{l,\mathrm{e}} + Q_h^{l,\mathrm{ESS}} - Q_h^{l,\mathrm{g}} \tag{25}$$

In the formula, $Q_h^{l,\mathrm{g}}$ represents the predicted output of the photovoltaic device of the user aggregator in the h-th time period within a day. $Q_h^{l,\mathrm{ESS}}$ represents the electrical energy stored or retrieved by the user aggregator from the shared energy storage system in the time period within a day, positive for storage and negative for retrieval. The positive and negative values of $Q_h^{l,\mathrm{c}}$ represent the electrical energy purchased/sold by the user aggregator from the micro-grid operator.

In the heating field, traditionally, users can only obtain thermal energy from micro-grid operators. However, with the advancement of electric heating technology, users can now use electric heating equipment

to meet all heat demand. Users can use these equipment to produce heat when the electricity price is low to increase revenue. Assuming that the user aggregator can manage the heat load within a day, the following constraint conditions are available:

$$Q_h^{l,\mathrm{h}} = \mu_h Q_h^{\mathrm{MGO,h}} + (1-\mu_h) Q_h^{u,\mathrm{h}} - \Delta Q_h^{l,\mathrm{h}} \tag{26}$$

$$0 \le \Delta Q_h^{l,\mathrm{h}} \le \Delta Q_{\max}^{l,\mathrm{h}} \tag{27}$$

In the formula, $Q_h^{u,\mathrm{h}}$ represents the thermal power provided by the user-side electric heating equipment of the user aggregator in the h-th time period within a day. $\Delta Q_h^{l,\mathrm{h}}$ and $\Delta Q_{\max}^{l,\mathrm{h}}$ represent the actual reduction and the maximum allowable reduction of the thermal load of the user aggregator in the h-th time period within a day, respectively. μ_h represents the coefficient of the user aggregator choosing the micro-grid operator as the heating side in the h-th time period within a day. A value of 0 indicates that the user uses electric heating equipment for heating, and a value of 1 indicates that the user purchases thermal energy from the micro-grid operator side.

The user-side electric heating response constraint conditions are expressed as:

$$Q_h^{u,\mathrm{h}} = \eta_{\mathrm{h}}^l \Delta Q_h^{l,\mathrm{e}} \tag{28}$$

$$0 \le Q_h^{u,\mathrm{h}} \le Q_{\max}^{u,\mathrm{h}} \tag{29}$$

$Q_h^{u,\mathrm{h}}$ is the user-side electric heating output in the h-th time period within a day. $Q_{\max}^{u,\mathrm{h}}$ is the maximum allowable heating output in the process of electric heating of the user aggregator. η_{h}^l is the comprehensive efficiency of user-side electric heating.

Comparing the two energy-obtaining methods of users, the selection plan of the heating coefficient μ_h is given:

$$\mu_h = \begin{cases} 0 & \text{if } \frac{\lambda_h^{MGO,s}}{\eta_h^l} + \theta \cdot e_{grid} \le \gamma_h^{MGO,s} + \theta \cdot e_{gas} \\ 1 & \text{otherwise} \end{cases} \tag{30}$$

The revenue of the user aggregator for a day is expressed as:

$$E_l = -E_l^{\mathrm{MGO,e}} + E_l^{\mathrm{u(e)}} - \left(E_l^{\mathrm{MGO,h}} + E_l^{\mathrm{ESS}}\right) - \sum_{h=1}^{H} \beta \Delta L_h^{l,\mathrm{h}^2} \tag{31}$$

In the formula, $E_l^{\mathrm{MGO,e}}$ represents the cost of electricity transactions between the user aggregator and the micro-grid operator, $E_l^{\mathrm{u(e)}}$ represents the electricity utility function of the user aggregator, $E_l^{\mathrm{MGO,h}}$ and E_l^{ESS} respectively represent the costs that the user aggregator needs to pay for purchasing thermal energy from the micro-grid operator and using the shared energy storage service; $\sum_{h=1}^{H} \beta \Delta L_h^{l,\mathrm{h}^2}$ represents the penalty cost for the decrease in comfort level due to the reduction of heat load by the user aggregator within a day. The above items can be further expressed as:

$$E_l^{\mathrm{u(e)}} = \sum_{h=1}^{H} \left(a \overline{Q_h^{l,\mathrm{e}}}^2 + b \overline{Q_h^{l,\mathrm{e}}} + c \right) \tag{32}$$

$$\overline{Q_h^{l,\mathrm{e}}} = Q_h^{l,\mathrm{f}} + \overline{Q_h^{l,\mathrm{s}}} + \Delta Q_h^{l,\mathrm{e}} + Q_h^{l,\mathrm{ESS}} \tag{33}$$

$$E_l^{\mathrm{ESS}} = F_+^{\mathrm{ESS}} \tag{34}$$

$$E_l^{\mathrm{MGO},e} = \sum_{h=1}^{H} \left[\lambda_h^{\mathrm{MGO},s} \cdot \max\left(L_h^{l,c}, 0\right) + \lambda_h^{\mathrm{EG,b}} \cdot \min\left(L_h^{l,\mathrm{c}}, 0\right) \right] \tag{35}$$

$$E_l^{\mathrm{MGO,h}} = E_{\mathrm{MGO}}^{l,\mathrm{h}} \tag{36}$$

Among them, $\overline{Q_h^{l,e}}$ represents the electrical load of the user aggregator after adjustment in the h-th time period within a day, and a, b, and c are the parameters of the user aggregator's electricity utility function.

2.1.4 Carbon Emission Trading and Power-Carbon Synergy Mechanism

To quantitatively integrate carbon emissions into the optimization framework, a carbon emission trading mechanism is explicitly formulated. The carbon emissions are primarily generated by the micro-gas turbine (MT). The daily carbon emission amount E_{carbon} (kg CO_2/day) is calculated based on the MT's fuel consumption and a carbon emission factor:

$$E_{\mathrm{carbon}} = \kappa_{\mathrm{carbon}} \cdot \sum_{h=1}^{H} C_{MT,h} \tag{37}$$

where $C_{MT,h}$ is the fuel cost of the micro-gas turbine in time period h (as defined in Eq. (3)), and κ_{carbon} is the carbon emission factor (kg CO_2/day), converting fuel cost to CO_2 emissions based on the fuel's carbon content and price.

The microgrid operator (MGO) participates in a cap-and-trade carbon market. The MGO is allocated a daily carbon emission quota Equota. The net carbon emission cost C_{carbon} is then incorporated into the MGO's overall cost function, creating a direct power-carbon synergy:

$$C_{\mathrm{carbon}} = \lambda_{\mathrm{carbon}} \cdot \left(E_{\mathrm{carbon}} - E_{\mathrm{quota}}\right) \tag{38}$$

where $\lambda_{\mathrm{carbon}}$ is the carbon price (¥/kg CO_2). This term Ccarbonis added to the MGO's total cost minimization objective (implicit in Eqs. (9)–(13). When $E_{carbon} > E_{quota}$, the MGO incurs a cost for purchasing additional allowances; conversely, if $E_{carbon} < E_{quota}$, it gains revenue by selling surplus allowances.

This mechanism inherently couples power dispatch with carbon emissions. Reducing reliance on the MT (e.g., by increasing wind/PV consumption) directly lowers E_{carbon}, reducing carbon costs or generating carbon credits. This synergy is reflected in the optimization outcomes presented in Section 3.

2.2 One-Stage Optimization-Game Strategy

2.2.1 Formal Stackelberg Game Formulation

The Stackelberg game $\Gamma = \left\{\mathrm{MGO}, L, S^{\mathrm{map}}, S^j, U^{\mathrm{map}}, U^j\right\}$ is defined where:

Leader (MGO): $\max U^m(\alpha, \gamma) = \mathrm{EMGO}$ (Eq. (12)) subject to (1) and (2).

Follower (L): $\max U^1(Q, P) = E^1$ (Eq. (32)) subject to (22)–(31).

The equilibrium existence follows from Rosen's existence theorem since:

Strategy sets $S^{\mathrm{M90}} = \left[\lambda^{\min}, \lambda^{\max}\right] \times \left[\gamma^{\min}, \gamma^{\max}\right]$ are convex and compact Payoff functions are concave in follower's variables and continuous in all variables The unique equilibrium is computed via backward induction using the best-response function:

$$\lambda^*, \gamma^* = argmax U^{\mathrm{map}}(\alpha, \gamma, Q(\alpha, \gamma)) \tag{39}$$

where $Q^*(\lambda, \gamma)$ is the follower's optimal response.

The micro-grid operator first formulates the set of electricity purchase price and heat purchase price strategies within a day, and then the user aggregator adjusts the electricity and heat loads in each period

in real-time according to the pricing plan of the micro-grid operator and the shared energy storage service lease fee, and rationally plans the use of shared energy storage services. The interaction variables between the micro-grid operator and the user aggregator are the selling electricity price, selling heat price, electricity purchase quantity, and heat purchase quantity [26]. When the micro-grid operator sets prices too high or too low, the user aggregator will dynamically adjust its electricity purchase quantity and heat purchase quantity. Conversely, the micro-grid operator will also re-formulate its pricing strategy based on the electricity purchase quantity and heat purchase quantity of the user aggregator until the optimal pricing strategy is found [27]. Obviously, there is a revenue conflict between the micro-grid operator and the user aggregator, and both sides have a sequential decision-making process. Therefore, the micro-grid operator and the user aggregator can be regarded as a principal-agent game model. This game R can be expressed as:

$$R = \left\{ \frac{(\mathrm{MGO} \cup l); \lambda^{\mathrm{MGO,b}}, \lambda^{\mathrm{MGO,s}},}{\overline{L_l^S}, \Delta L^{l,h}, \Delta L^{l,wind}, L^{l,\mathrm{ESS}}; E_{\mathrm{MGO}}; E_l} \right\} \tag{40}$$

In the model, the micro-grid operator MGO is the leader, and the user aggregator l is the follower. $\overline{L_l^S}$ represents the set of flexible load strategies of the user aggregator after adjustment within a day. $\Delta L^{l,h}$ represents the set of strategies for the user aggregator to reduce heat energy within a day. $\Delta L^{l,wind}$ represents the set of strategies for the user aggregator to utilize wind-power generation within a day. $L^{l,\mathrm{ESS}}$ represents the set of strategies for the user aggregator to use shared energy-storage services within a day. E_l represents the revenue of the user aggregator within a day. $\lambda^{\mathrm{MGO,b}}$ and $\lambda^{\mathrm{MGO,s}}$ respectively represent the sets of strategies for the micro-grid operator's purchase price and selling price within a day. E_{MGO} represents the revenue of the micro-grid operator within a day.

2.2.2 Solution Methods

The equilibrium existence follows from concave payoff functions and compact strategy sets. Uniqueness is ensured by the strict concavity of follower's objective. The bilevel optimization is solved via backward induction, where the leader anticipates follower's best response.

The solution methods for the first-stage game model are as follows:

(1) Search space: Search the entire strategy space by traversing all strategy combinations to find potential optimal solutions.

(2) Discretization processing: Discretize the strategies. Next, it is proved through theoretical derivation that a Nash equilibrium point exists for this game problem in the continuous strategy set [28], and it is further proved that there is also a Nash equilibrium point after the discretization of the finite strategy set to ensure traversal feasibility.

(3) Confirmation of Nash equilibrium point: According to the definition of pure-strategy Nash equilibrium, combined with this game model, it can be obtained that: when all game—side strategy sets are $[0, +\infty)$, point ; $P0\ (ai, bd)$ is the pure-strategy Nash equilibrium point of the above-mentioned game problem, $a_i = (d_\mathrm{b} + d_\mathrm{s})/2$, $b_\mathrm{d} = (d_\mathrm{s} - d_\mathrm{b})/2$. For continuous finite strategy sets, due to the reason of the upper limit of the market—specified quotation, at this time, the strategy sets are $[0, a_{i,\max}]$ and $[0, b_{\mathrm{d,max}}]$, and still satisfy $a_i = (d_\mathrm{b} + d_\mathrm{s})/2$, $b_\mathrm{d} = (d_\mathrm{s} - d_\mathrm{b})/2$, and the Nash equilibrium point is still P0. For discrete finite strategy sets, discrete intervals are set, and discrete processing is carried out according to the formula. According to the determined strategy upper-limit values and the Nash equilibrium existence theorem, Nash equilibrium still exists. The upper-limit satisfies $a_{i,\max} \geq$

$(d_b + d_s)/2$, $b_{d,max} \geq (d_s - d_b)/2$, and $P0$ is still the pure-strategy Nash equilibrium point.

$$\begin{cases} a_i = k_i \Delta c_i & k_i \in Z^+ \\ b_d = k_d \Delta s_d & k_d \in Z^+ \end{cases} \tag{41}$$

The system has chosen different operation modes under different strategy combinations, and has realized the optimal scheduling of each micro-grid in the game optimization.

2.3 Two-Stage Optimization—Stochastic Robust Optimization Model

2.3.1 Objective Function

In the second stage, a stochastic robust optimization model is constructed, with the objective of minimizing the operating cost. The objective function is constructed based on the construction of a typical micro-grid system.

The objective function mainly considers two parts: investment cost and operating cost. Among them, the investment cost is mainly the annual equivalent investment cost of energy storage, and the operating cost includes the interactive cost of the distribution network (the cost of electricity purchase and sale), the operation and maintenance cost of each unit, and the fuel cost of the micro-gas turbine.

$$\min C = \min \left\{ C_{\text{int}} + C_{ope} \right\} \tag{42}$$

$$\begin{cases} C_{\text{int}} = \frac{\rho(1+\rho)^{r_{bat}}}{(1+\rho)^r - 1} * c_{BAT.\text{int}} E_{BAT.\max} + C_{-}^{\text{ESS}} \\ C_{ope} = \sum_{i=1}^{I} 365 k_i \left[C_{BAT.i} + C_{GRID.i} + C_{OM.i} + C_{MT.i} + C_{WIND.i} \right] \end{cases} \tag{43}$$

$$\begin{cases} C_{GRID.i} = \sum_{t=1}^{24} \left[c_{GRID}(t) P_{\text{buy.i}}(t) \Delta t - c_{GRID}(t) P_{\text{sell.i}}(t) \Delta t \right] \\ C_{OM.i} = \sum_{W}^{W} \sum_{t=1}^{24} c_{OM.W} P_{W.i}(t) \Delta t \\ C_{MT.i} = \sum_{t=1}^{24} c_{MT} P_{G.i}(t) \Delta t \end{cases} \tag{44}$$

In the formula, C is the comprehensive cost, C_{int} is the annual equivalent investment cost of energy storage, and C_{ope} is the annual operation cost of the micro-grid. ρ is the discount rate, r is the number of discount years, $c_{BAT.\text{int}}$ is the investment cost per unit capacity of energy storage, and $E_{BAT.\max}$ is the maximum configuration capacity of energy storage. $P_{\text{buy.i}}$ is the purchase price, $P_{\text{sell.i}}(t)$ is the selling price, $C_{BAT.i}$, $C_{GRID.i}$, $C_{OM.i}$, $C_{MT.i}$, $C_{WIND.i}$ are respectively the daily-life loss cost of energy storage, the cost of electricity purchase and sale, the operation and maintenance cost of each unit, the fuel cost, and the wind cost corresponding to the i-th typical day. c_{GRID} is the electricity price of the power grid, and $c_{OM.W}$ is the operation and maintenance cost coefficient of the W-th type of unit.

Without considering the uncertainties of photovoltaic output and load power, a deterministic optimization model for the economic dispatch problem of the micro-grid is obtained, and its compact form is as follows:

$$\begin{cases} \min_{x,y} \quad c^{\text{T}} y \\ \text{s.t. } Dy \geq d \\ Ky = 0 \\ Fx + Gy \geq h \\ I_u y = \hat{\mathbf{u}} \end{cases} \tag{45}$$

In the formula, x and y are variables that need to be optimized, and the specific expressions are:

$$\begin{cases} x = \left[\mu_h,\ Q_h^{l,\mathrm{ESS}}\right]^{\mathrm{T}} \\ y = \left[c_{\mathrm{BAT,int}},\ E_{\mathrm{BAT,max}},\ P_{\mathrm{buy},i},\ P_{\mathrm{sell},i}(t),\ C_{\mathrm{BAT},i},\ C_{\mathrm{GRID},i},\ C_{\mathrm{OM},i},\ C_{\mathrm{MT},i},\ C_{\mathrm{WIND},i},\ c_{\mathrm{GRID}},\ c_{\mathrm{OM,W}}\right]^{\mathrm{T}} \\ \mathbf{t} = (1, 2, \cdots, N_{\mathrm{T}}) \end{cases} \tag{46}$$

The vector c corresponds to the cost minimization; the matrices D, K, F, G, and I_{u} correspond to the variables under constraint conditions; the vectors d, h are constant vectors. The values of photovoltaic output and load power are the predicted values for each period, among which:

$$\hat{\mathbf{u}} = \left[\hat{u}_{\mathrm{Pr}}(t), \hat{u}_R(t)\right]^{\mathrm{T}}, \quad t = (1, 2 \cdots N_{\mathrm{T}}) \tag{47}$$

In the equation, $\hat{u}_{\mathrm{Pr}}(t)$ and $\hat{u}_R(t)$ respectively represent the predicted values of photovoltaic output and load power in period t.

In the operation of micro-grids, affected by many random factors, it is difficult to ensure the prediction accuracy. Considering that the range of photovoltaic output and load power should be in the uncertainty set, the equations are as follows:

$$U = \begin{cases} \mathbf{u} = \left[u_{\mathrm{PV}}(t), u_{\mathrm{L}}(t)\right]^{\mathrm{T}} \in \mathbb{R}^{(N_{\mathrm{T}})\times 2}, t = 1, 2 \cdots N_{\mathrm{T}} \\ u_{\mathrm{PV}}(t) \in \left[\hat{u}_{\mathrm{PV}}(t) - \Delta u_{\mathrm{PV}}^{\max}(t), \hat{u}_{\mathrm{PV}}(t) + \Delta u_{\mathrm{PV}}^{\max}(t)\right] \\ u_{\mathrm{L}}(t) \in \left[\hat{u}_{\mathrm{L}}(t) - \Delta u_{\mathrm{L}}^{\max}(t), \hat{u}_{\mathrm{L}}(t) + \Delta u_{\mathrm{L}}^{\max}(t)\right] \end{cases} \tag{48}$$

$u_{\mathrm{PV}}(t)$ and $u_{\mathrm{L}}(t)$ represent the introduced uncertain photovoltaic output and load power uncertain variables; $\Delta u_{\mathrm{PV}}^{\max}(t)$ and $\Delta u_{\mathrm{L}}^{\max}(t)$ respectively represent the maximum fluctuation deviations allowed for photovoltaic output and load power.

The construction of the operation optimization model aims to find the optimal scheduling plan with the best economy when the uncertain variable u changes towards the worst-case scenario within the uncertainty set U, which has the following form:

$$\begin{cases} \min_x \left\{\max_{u\in U} \min_{y\in\Omega(x,u)} \mathbf{c}^{\mathrm{T}} y\right\} \\ \text{s.t.} x = (x_1, x_2, \cdots, x_{2\times N_{\mathrm{T}}})^{\mathrm{T}} \\ x_i \in \{0, 1\}, \forall i \in (1, 2, \cdots 2 \times N_{\mathrm{T}}) \end{cases} \tag{49}$$

In the equation, the outer-layer minimization is the first-layer problem, and the optimization variable is x; the inner-layer maximization-minimization is the second-layer problem, and the optimization variables are u and y. For the uncertain variable, it can be simplified into the above deterministic optimization model. The purpose of the max structure in the optimization problem is to find the worst-case scenario with the largest operation cost.

Given a set of $O(x, u)$ optimization variables y feasible region, the formula is as follows:

$$O(x, u) := \begin{Bmatrix} y| & \\ Dy \geq d, & \to y \\ Ky = 0, & \to \lambda \\ Fx + Gy \geq h, & \to v \\ I_{\mathrm{u}} y = u. & \to \pi \end{Bmatrix} \tag{50}$$

γ, λ, ν, π represent the dual variables corresponding to each constraint in the minimization problem.

2.3.2 Solution Algorithm

The second-stage optimization problem is solved using the C&CG algorithm. Compared with the Benders algorithm, the C&CG algorithm can continuously add relevant variables and constraints of sub-problems when solving the master problem, thereby increasing the dimension of the space and obtaining a tighter lower bound of the original objective function value, thus effectively reducing the number of iterations.

The form of the master problem is established as follows:

$$\begin{cases} \min_x \ \alpha, \\ \text{s.t. } \alpha \geq c^{\mathrm{T}} y_t \\ D y_t \geq d \\ K y_t = 0 \\ F x + G y_t \geq h \\ I_u y_t = u_t^* \\ \forall l \leq k \end{cases} \tag{51}$$

In the formula, k is the current iteration number, y_t is the solution of the sub-problem after the l-th iteration, and u_t^* is the value of the uncertain variable u obtained after the l-th iteration under the worst-case scenario.

The form of the sub-problem after decomposition is

$$\max_{u \in U} \min_{y \in \Omega(x,u)} c^{\mathrm{T}} y \tag{52}$$

The minimization of the inner layer in the above formula under the given (x, u) is a linear problem. According to the strong duality theory and the corresponding relationship, it is transformed into the max form and combined with the outer max problem to obtain the following dual problem:

$$\begin{cases} \max_{u \in U, \gamma, \lambda, \nu, \pi} d^{\mathrm{T}} \gamma + (h - Fx)^{\mathrm{T}} \nu + u^{\mathrm{T}} \pi \\ \text{s.t.} D^{\mathrm{T}} \gamma + K^{\mathrm{T}} \lambda + G^{\mathrm{T}} \nu + I_{\mathrm{u}}^{\mathrm{T}} \pi \leq c \\ \gamma \geq 0, \nu \geq 0, \pi \geq 0 \end{cases} \tag{53}$$

There are non-convex bilinear terms $u^{\mathrm{T}} \pi$ in this formula, and it is rather difficult to solve them using a solver. Therefore, an improved AOP algorithm is used for solution. The AOP algorithm decomposes the nonlinear problem into smaller-scale sub-problem forms and iteratively solves them to obtain an approximate solution to the original problem.

By introducing auxiliary variables and relevant constraints for linearization, we can obtain:

$$\begin{aligned} &A\text{: } W \leftarrow \sum_{t=1}^{N_{\mathrm{T}}} B_{\mathrm{PV}} \leq \Gamma_{\mathrm{PV}} \\ &B\text{: } W' \leftarrow \sum_{t=1}^{N_{\mathrm{T}}} B_{\mathrm{L}} \leq \Gamma_{\mathrm{L}} \\ &\pi - \overline{\pi}(1 - B) \leq B' \leq \pi \end{aligned} \tag{54}$$

Δu and $\mathbf{B}$ are the introduced continuous auxiliary variables, and $\overline{\pi}$ is the upper bound of the dual variable.

A smart energy-load scheduling method is described as follows. Its characteristic is that the AOP algorithm is used for solution. The flowchart of the solver is shown in Fig. 3. The AOP algorithm flow is as follows:

(1) Initialization: Given the initial uncertain variable u, it can be its predicted value.
(2) Setting upper and lower bounds: Set the lower bound of the operation cost corresponding to the final scheduling plan as $LB = -\infty$ and the upper bound as $UB = +\infty$;
(3) Algorithm improvement and optimization: Optimize the search step size,

$$R = i \times e^{-(\beta \times g)/Maxge} \tag{55}$$

i is the step-length control factor, β is the exponential control factor, g is the current iteration number, and $Maxge$ is the maximum iteration number.
(4) Iterative solution: Solve sub-problem A. If $W < \infty$, then update the dual variable and output W; solve sub-problem B and update u as the given value for the next iteration, and output W';
(5) Convergence test: If $|W' - W|/W \leq \tau$, then the algorithm converges, and return to step 2. τ is the convergence tolerance, taken as 10^{-3};

The characteristics of the above derivation and transformation lie in using the C&CG algorithm for solution. The C&CG algorithm flow is as follows:

(1) Given the initial value u as the worst-case scenario, set the lower bound of the operation cost corresponding to the final scheduling plan as $LB = -\infty$, the upper bound as $UB = +\infty$, and the iteration number $k = 2$;
(2) Solve the main problem: Substitute $u1^*$ into the main problem to obtain the optimal solution $\left(x_k^*, \alpha_k^*, y^{1*}, \cdots, y^{k^*}\right)$ and update the lower bound $LB = \alpha_k^*$;
(3) Solve the sub-problem: Substitute the obtained main problem solution x_k^*; into the formula, combine with the AOP algorithm, solve to obtain the values of the objective function and the uncertain variables under the worst-case scenario corresponding to the sub-problem, and update the upper bound.
(4) Convergence detection and output: When $(UB - LB)/UB \leq \varepsilon$, the algorithm converges, output the objective function values and the optimal solution x^l, u_k^{l+1}, y_k^l otherwise, jump back to step (2). The main problem adds sub-problem variables and corresponding constraint conditions to continue the cycle until the algorithm converges.

The computational efficiency of the proposed improved AOP algorithm within the C&CG framework was evaluated on a standard PC with an Intel i7-12700H processor and 16GB RAM. For the 24-h scheduling horizon of the case study microgrid, the average solution time was 285 s, with the algorithm typically converging within 12 iterations. This demonstrates the tractability of the approach for day-ahead scheduling applications.

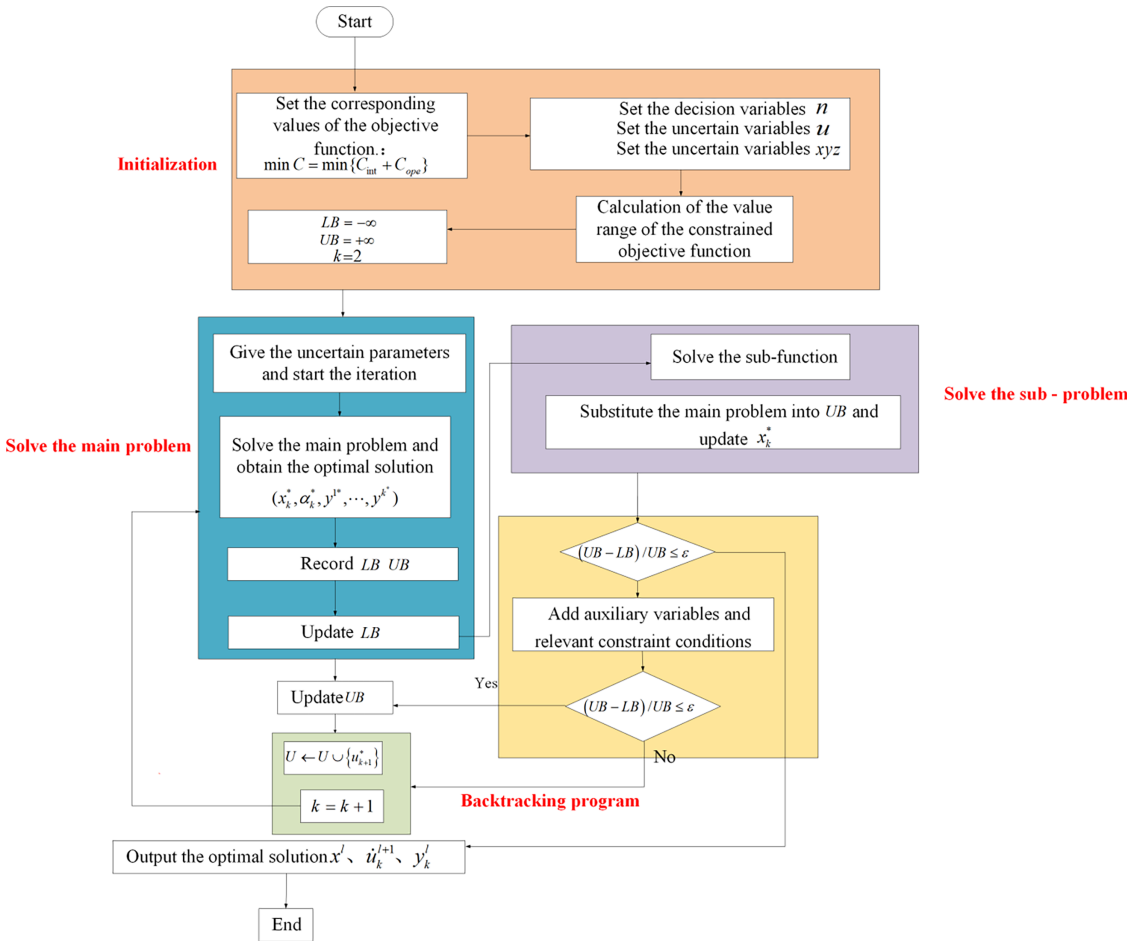

Figure 3: Flowchart of the solver.

2.4 Impact of Source-Load Disturbance on the System

Load-Loss Probability

The power supply reliability of the system is an indicator for evaluating the robustness of the system under adverse scenarios. The load-loss probability [29] is used to evaluate the robustness of the integrated energy micro-grid. The formula is as follows:

$$R_{LPSP} = \frac{\sum_{t=1}^{T} Q_{shortage,t}}{\sum_{t=1}^{T} Q_{nowload,t}} \tag{56}$$

R_{LPSP} represents the load-loss probability coefficient, $Q_{shortage,t}$ represents the load-shortage quantity at time, and $Q_{nowload,t}$ represents the load-receiving quantity at time.

3 Case Analysis

3.1 Parameter and Scenario Settings

To assess the effectiveness and rationality of the proposed two-stage robust source-load optimal scheduling strategy based on game-theoretic mechanisms, this study employs a case study of a large-scale residential community located in northern Jiangsu, China. The community is equipped with a diverse set of energy generation and management technologies, including photovoltaic (PV) power generation systems (150 kW capacity), electric heating and cooling devices (700 kW capacity), micro-gas turbines (950 kW capacity), and wind power generation systems (200 kW capacity). The load operation data are analyzed with a one-hour sampling interval over a 24-h scheduling period. The shared energy storage service provider charges a daily lease fee of 0.33 yuan per kWh. The user-side flexible load is characterized by a flexibility proportion (p) of approximately 10%, with a flexibility coefficient of 0.2 yuan per kW^2. The thermal load is bounded by upper and lower limits of 0.5 kW per yuan and 0.15 kW per yuan, respectively.

To further investigate the impact of the two-stage robust source-load optimization scheduling based on game-theoretic strategies on community-based integrated energy microgrids, six distinct scenarios are established for comparative analysis.

Case 1: No game mechanism is considered, and energy storage is applied solely to the consumption of renewable energy in the community.

Case 2: No game mechanism is considered, and energy storage is applied to multiple scenarios, including the consumption of renewable energy in the community, peak shaving and valley filling, and market trading.

Case 3: The game mechanism is considered, and energy storage is applied solely to the consumption of renewable energy in the community.

Case 4: The game mechanism is considered, and energy storage is applied to multiple scenarios, including the consumption of renewable energy in the community, peak shaving and valley filling, and market trading.

Case 5: Both the game mechanism and the power-carbon synergy mechanism are considered, and energy storage is applied solely to the consumption of renewable energy in the community.

Case 6: Both the game mechanism and the power-carbon synergy mechanism are considered, and energy storage is applied to multiple scenarios, including the consumption of renewable energy in the community, peak shaving and valley filling, and market trading.

3.2 Comparison of Optimization Operation Results under Different Scenarios

For the 6 scenarios that have been set, solutions are obtained according to the robust optimization model established in this paper. The optimization operation results under different scenarios are shown in Table 1, and the output curves of the optimized system are shown in the figure.

To ensure a fair and transparent comparison, the six cases are defined based on the activation of three key mechanisms: (1) the Game-theoretic mechanism (GT), representing the Stackelberg game between the MGO and the aggregator; (2) the Power-Carbon Synergy mechanism (PCS), which incorporates the carbon trading cost into the MGO's objective function; and (3) the Energy Storage Application Scenarios (ES), where 'Single' denotes storage is used only for renewable energy consumption, and 'Multiple' includes additional applications in peak shaving, valley filling, and market trading. The specific configuration for each case is summarized in Table 2 below.

Table 1: Comparison of optimization results in different scenarios.

Case	Daily Cost/Yuan	Energy Storage Revenue/Yuan	Wind Power Consumption Rate/%	Photovoltaic Power Consumption Rate/%
1	6733	99.6	79.66	78.91
2	6221	301.4	84.21	85.43
3	6233	129.7	86.45	86.63
4	5721	426.3	89.67	91.98
5	5789	256.1	94.36	95.96
6	4965	658.2	98.76	98.91

Table 2: Case configuration definition.

Case	Game Mechanism (GT)	Power-Carbon Synergy (PCS)	Storage Scenarios (SS)
Case 1	Inactive	Inactive	Single
Case 2	Inactive	Inactive	Multiple
Case 3	Active	Inactive	Single
Case 4	Active	Inactive	Multiple
Case 5	Active	Active	Single
Case 6	Active	Active	Multiple

Furthermore, key metrics are explicitly defined as follows:

Daily Cost (Yuan): The total daily operational cost for the Microgrid Operator (MGO), encompassing electricity purchase/sale, fuel costs, operation maintenance, and, when active, the carbon emission cost.

Energy Storage Revenue (Yuan): The net revenue of the Shared Energy Storage Operator, calculated as $C^{\mathrm{ESS}} = C_{+}^{\mathrm{ESS}} - C_{-}^{\mathrm{ESS}}$ from Eqs. (20) and (21), representing income from leasing fees minus charging/discharging costs.

Wind/PV Accommodation Rate (%): The percentage of available wind/PV generation that is successfully consumed within the microgrid or sold to the main grid, calculated as Accommodation

$$\text{Accommodation Rate} = \left(1 - \frac{\text{Curtailed Energy}}{\text{Available Energy}}\right) \times 100\%$$

As indicated in Table 1, Case 6, which incorporates both the game mechanism and the power-carbon synergy mechanism, along with the multi-scenario application of energy storage, achieves the lowest daily operational cost of 4965 yuan and the highest energy storage revenue of 658.2 yuan. Additionally, Case 6 realizes the highest consumption rates of wind and photovoltaic energy at 98.76% and 98.91%, respectively. In contrast, Case 1, which does not consider either mechanism, exhibits the highest total cost of 6733 yuan.

Fig. 4 illustrates the operational characteristics of various scenarios, highlighting the impact of different strategies on system performance. In Case 1, where neither the game mechanism nor the power-carbon synergy mechanism is considered, and energy storage is solely applied to renewable energy consumption, the system primarily relies on wind power and gas turbines for electricity supply during the low-load period from 0:00 to 6:00, with energy storage performing charging and discharging operations. However, the single application scenario limits scheduling flexibility and economic efficiency. During the photovoltaic (PV)

generation period from 6:00 to 18:00, especially during the peak period from 10:00 to 12:00, the storage strategy restricts the system's ability to sell electricity to the grid despite high electricity prices, thereby reducing revenue. Overall, Case 1 underperforms compared to Case 4, which employs energy storage in multiple scenarios, in terms of cost, energy storage revenue, and renewable energy consumption rates.

In Case 2, energy storage is applied in multiple scenarios, including renewable energy consumption, peak shaving, valley filling, and market trading, without considering the game mechanism. The system again relies on wind power and gas turbines for electricity supply during the 0:00 to 6:00 period, with energy storage performing charging and discharging operations. This approach enhances scheduling flexibility and economic efficiency. During the PV generation period from 6:00 to 18:00, the energy storage system can schedule more flexibly and sell electricity to the grid to generate revenue. Consequently, Case 2 outperforms Case 1 in terms of cost, energy storage revenue, and renewable energy consumption rates. However, it still falls short compared to Case 4, which incorporates the game mechanism.

Case 3 considers the game mechanism but applies energy storage solely to renewable energy consumption. Similar to Case 1, the system relies on wind power and gas turbines for electricity supply during the low-load period from 0:00 to 6:00, with energy storage performing charging and discharging operations. The game mechanism enhances scheduling flexibility and economic efficiency to some extent. However, during the PV generation period from 6:00 to 18:00, the storage strategy continues to restrict the system's ability to sell electricity to the grid despite high prices. Overall, Case 3 underperforms Case 4 in terms of cost, energy storage revenue, and renewable energy consumption rates, although the game mechanism provides some improvement in economic efficiency.

Case 4, which considers the game mechanism and applies energy storage in multiple scenarios (renewable energy consumption, peak shaving, valley filling, and market trading), demonstrates superior performance. The system relies on wind power and gas turbines for electricity supply during the low-load period from 0:00 to 6:00, with energy storage performing charging and discharging operations. This approach significantly enhances scheduling flexibility and economic efficiency. During the PV generation period from 6:00 to 18:00, the energy storage system can schedule more flexibly and sell electricity to the grid to generate revenue. Consequently, Case 4 performs well in terms of cost, energy storage revenue, and renewable energy consumption rates, with the game mechanism and multi-scenario application significantly improving economic efficiency and flexibility.

Case 5 incorporates both the game mechanism and the power-carbon synergy mechanism but applies energy storage solely to renewable energy consumption. Similar to Cases 1 and 3, the system relies on wind power and gas turbines for electricity supply during the low-load period from 0:00 to 6:00, with energy storage performing charging and discharging operations. The game and power-carbon synergy mechanisms enhance scheduling flexibility and economic efficiency. However, during the PV generation period from 6:00 to 18:00, the storage strategy still restricts the system's ability to sell electricity to the grid despite high prices. Overall, Case 5 underperforms Case 6 in terms of cost, energy storage revenue, and renewable energy consumption rates, although the game and power-carbon synergy mechanisms provide some improvement in economic efficiency.

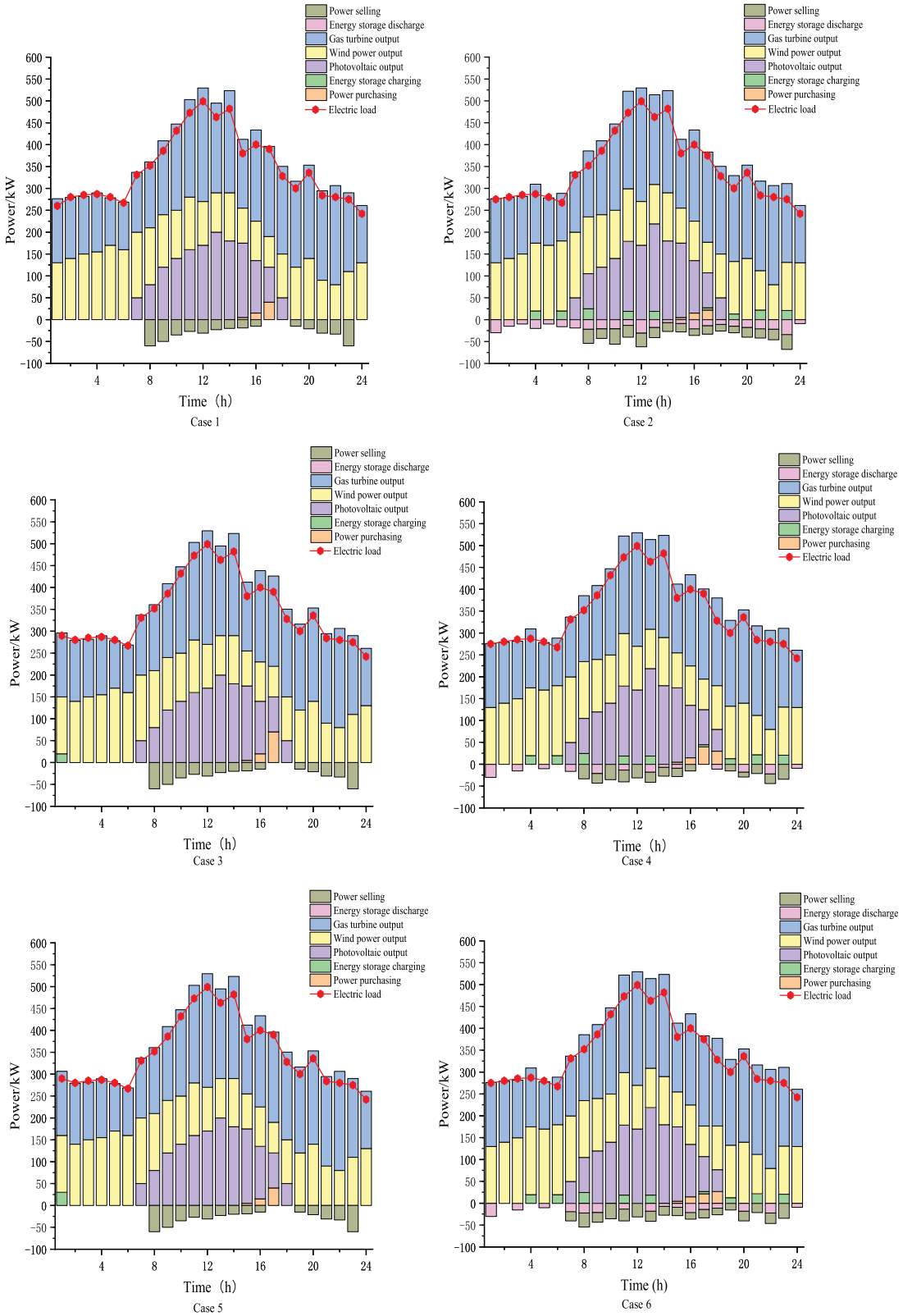

Figure 4: The output curve of the optimized system.

Case 6, which considers both the game mechanism and the power-carbon synergy mechanism and applies energy storage in multiple scenarios, demonstrates the best overall performance. The system relies on wind power and gas turbines for electricity supply during the low-load period from 0:00 to 6:00, with energy storage performing charging and discharging operations. This approach significantly enhances scheduling flexibility and economic efficiency. During the PV generation period from 6:00 to 18:00, the energy storage system can schedule more flexibly and sell electricity to the grid to generate revenue. Consequently, Case 6 performs well in terms of cost, energy storage revenue, and renewable energy consumption rates, with the game and power-carbon synergy mechanisms and multi-scenario application significantly improving economic efficiency and flexibility.

To visually demonstrate the enhanced accommodation of renewable energy, particularly in optimal scenarios like Case 6, the output curves before and after the optimization are compared in Fig. 5. The figure clearly shows a significant reduction in wind and PV power curtailment after the implementation of the proposed strategy, corroborating the high accommodation rates reported in Table 1.

In summary, Cases 4 and 6 achieve the best performance in terms of cost, energy storage revenue, and renewable energy consumption rates. These cases benefit from the integration of both the game mechanism and the power-carbon synergy mechanism, as well as the application of energy storage in multiple scenarios. In contrast, Cases 1 and 3, which employ single application scenarios, perform relatively poorly. Cases 2 and 5 show some improvement in economic efficiency and flexibility but still underperform compared to Cases 4 and 6.

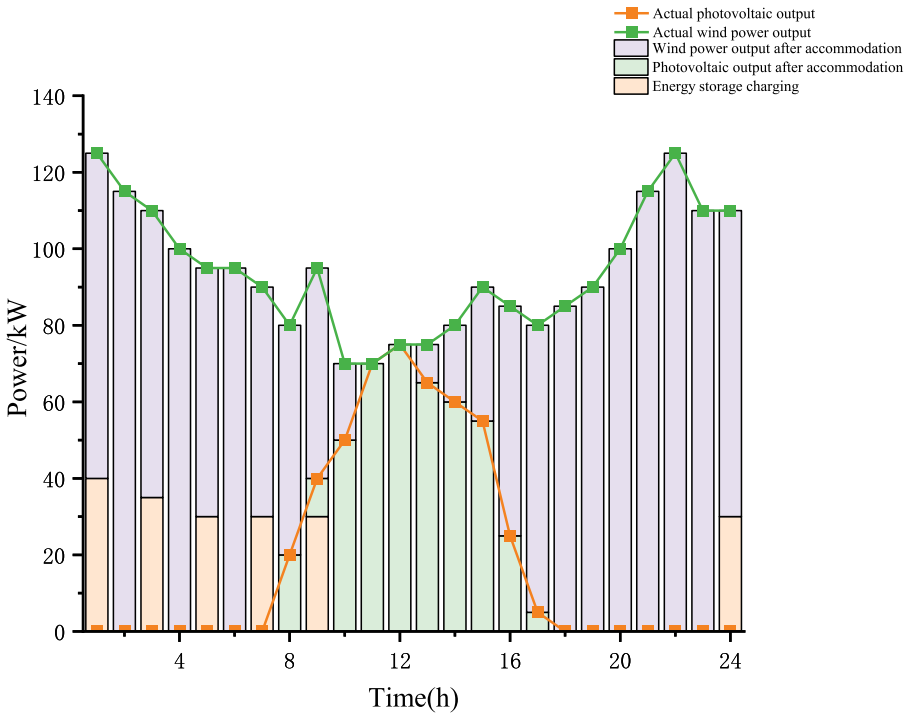

Figure 5: Before and after the accommodation of renewable energy.

The comparative analysis, supported by the clear definitions in Table 2, allows for a direct attribution of performance improvements. The reduction in daily cost from Case 1 to Case 2 is primarily driven by the multi-scenario application of energy storage, which enhances arbitrage opportunities. The introduction of the game-theoretic mechanism (Case 3 vs. Case 1, and Case 4 vs. Case 2) enables more dynamic pricing

and load adjustment, leading to further cost optimization and higher renewable accommodation. The most significant improvement in Case 6 is a synergistic result of combining all three active mechanisms: the GT mechanism optimizes economic interactions, the PCS mechanism incentivizes low-carbon dispatch, and the multi-scenario ES provides the necessary flexibility to achieve these goals efficiently.

3.3 Sensitivity Factor Analysis

Under the Case 6 scenario, a comparison was made between the robust optimization model and the deterministic model by selecting four random days.

As depicted in Fig. 6, the robust optimization model exhibits higher operational costs compared to the deterministic model. This elevated cost profile is attributable to the model's consideration of potential disturbances within the system. Specifically, the robust optimization model accounts for worst-case scenarios associated with three types of disturbances: wind power, photovoltaic (PV) generation, and load variations. These considerations, while increasing operational costs, also enhance the system's resilience. Within the same day, the robust optimization model achieves significantly lower load curtailment compared to the deterministic model, thereby demonstrating superior power supply reliability under adverse conditions. Moreover, the robust optimization model attains a higher energy supply efficiency ratio on the same day, indicating enhanced resilience against disturbances.

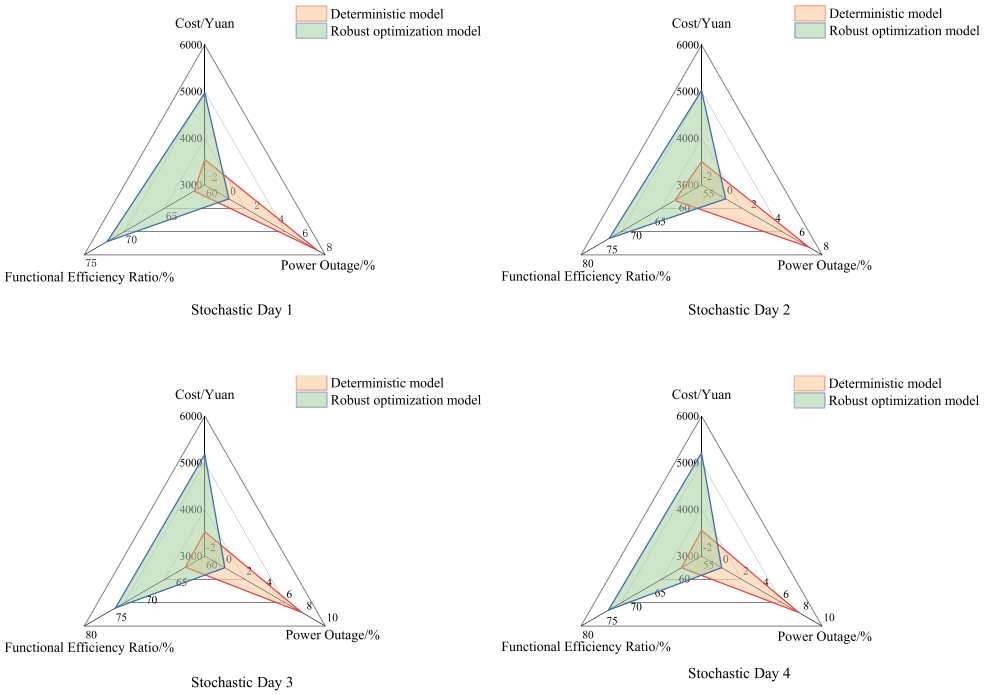

Figure 6: Long-term cost and load power-outage rate.

The influence of the interference coefficient on the total system cost is illustrated in Fig. 7.

As illustrated in Fig. 8, the carbon emissions of each scenario vary significantly. Case 6, which incorporates the power-carbon synergy mechanism, the game mechanism, and integrated community load scenarios, exhibits carbon emissions of 1673 kg CO_2/day, while Case 1, which lacks these mechanisms, has the highest emissions of 3294 kg CO_2/day. The average daily carbon emissions for Cases 1 to 6 are 3294,

2667, 2478, 2236, 1964, and 1673 kg, respectively. Compared to Case 1, Case 6 achieves a carbon emission reduction of approximately 49.2%. This significant reduction underscores the effectiveness of integrating the game mechanism and power-carbon synergy mechanism into the scheduling scheme. The carbon trading mechanism is modeled by incorporating a carbon price (λ_{carbon}) into the microgrid operator's cost function, where the carbon cost is proportional to the excess emissions beyond a baseline quota, aligned with regional carbon market regulations.

In the community energy microgrid employing this optimized scheduling approach, the system's compatibility with green energy has been notably enhanced. The green energy penetration rate has reached 53.91%, surpassing the previous threshold of 50%. This improvement is attributed to the implementation of the two-stage robust optimization scheduling, which has also increased system stability by 53.1%. These results highlight the importance of adopting advanced scheduling strategies to enhance the sustainability and reliability of community energy microgrids.

To further investigate the robustness of the power-carbon synergy mechanism, a sensitivity analysis was conducted on the carbon price. The carbon price (λ_{carbon}) was varied from 0 to 1.0 CNY/kg CO_2, while keeping other parameters constant in Case 6 (the optimal scenario). The results indicate that as the carbon price increases, the microgrid operator's total cost rises due to higher carbon penalties, but the carbon emissions decrease monotonically. For instance, at λ_{carbon} = 0.5 CNY/kg CO_2, the daily carbon emissions reduce to 1500 kg CO_2/day, while the operational cost increases by 8.5%. This analysis demonstrates that the proposed model is sensitive to carbon price fluctuations, and higher carbon prices incentivize greater renewable energy integration. The sensitivity results align with typical carbon market behaviors, providing practical insights for policymakers.

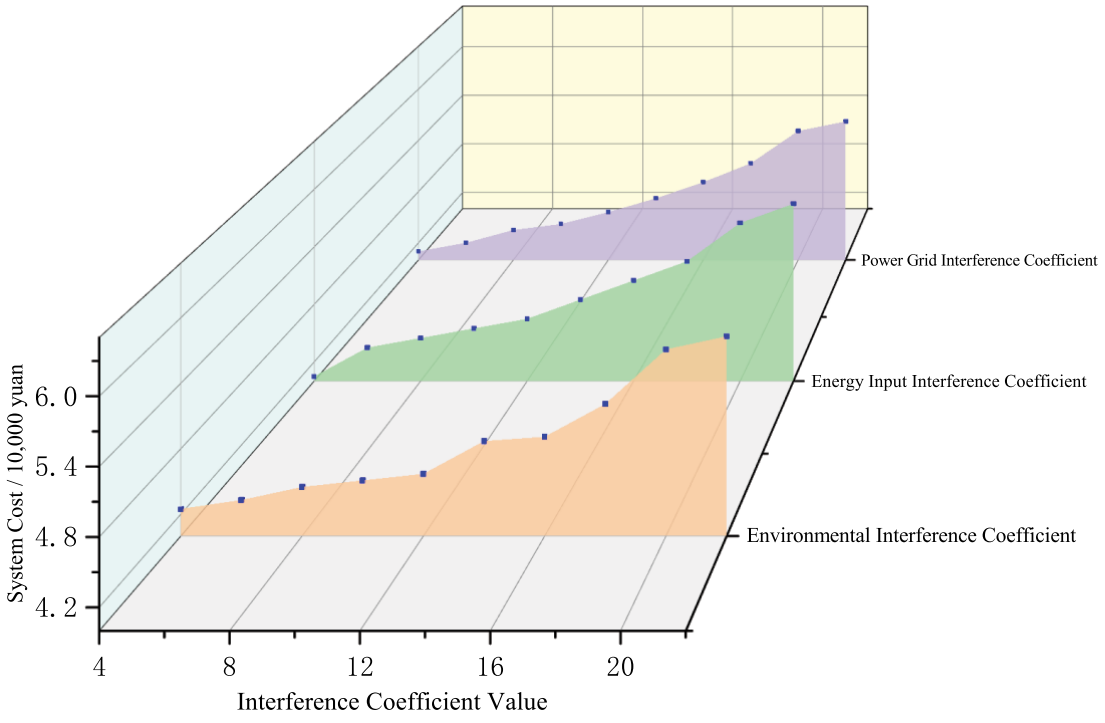

Figure 7: Diagram of interference coefficient.

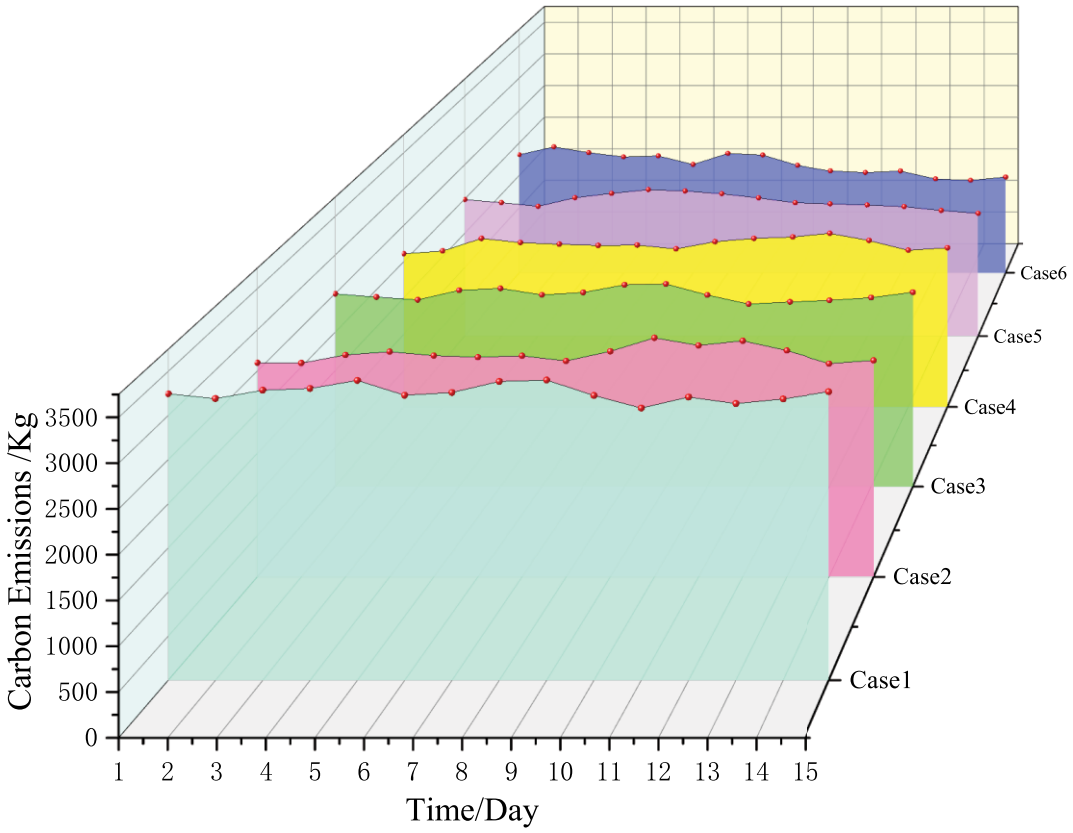

Figure 8: Long-term carbon emission diagram.

3.4 Robustness Test

To validate the robustness of the proposed scheduling plan against source-load uncertainties, a Monte Carlo simulation with 500 samples is conducted. The uncertainty modeling for the simulation is designed to be conservative and computationally efficient. While wind power forecast uncertainty is derived from a Weibull distribution in the planning model, for the purpose of testing the feasibility of the day-ahead schedule under extreme deviations, the PV output and load demand forecasting errors are modeled using bounded uncertainties sampled from a standard normal distribution, truncated at the 3σ confidence intervals referenced in Eq. (51). This approach stress-tests the schedule against large, albeit less likely, deviations.

The feasibility of each scenario is evaluated primarily using the Loss of Power Supply Probability (LPSP) index, calculated as Eq. (56). A scenario is deemed infeasible if $R_{LPSP} \geq 5\%$. This criterion serves as a proxy for system-level security constraints. A high LPSP indicates a significant power imbalance, which, in a real distribution network, would inevitably lead to security violations such as frequency excursions and voltage deviations beyond acceptable limits [30]. This study focuses on the energy balance and economic feasibility of the schedule provided by the GT-RO-PCC paradigm. Therefore, the LPSP provides a sufficient and direct metric to assess the robustness of the schedule against energy inadequacy. The deterministic optimization model, which relies on forecasted values, fails to account for these uncertainties, resulting in a high number of infeasible scenarios as shown in Table 3. In contrast, the proposed robust optimization model proactively internalizes uncertainty, achieving zero infeasible scenarios and demonstrating its superior ability to maintain a secure and reliable power supply under adverse conditions.

Table 3: Monte Carlo simulation status under different scenarios.

The Number of Infeasible Scenarios						
Case	**Case 1**	**Case 2**	**Case 3**	**Case 4**	**Case 5**	**Case 6**
Deterministic model	491	493	495	497	500	500
Robust optimization model	0	0	0	0	0	0

Table 3 reveals that the robust optimization approach does not encounter infeasible scenarios, demonstrating its robustness against future source-load fluctuations. To further validate the operational stability under uncertainty, we analyzed key intermediate metrics from the feasible Monte Carlo scenarios. As illustrated in Fig. 9, the robust optimization model significantly reduces real-time market imbalances compared to the deterministic model. Quantitative analysis shows that the standard deviation of the daily operating cost across all 500 scenarios for the robust model was only ¥185.2, which is 68% lower than that of the deterministic model (¥582.7). This indicates a much more stable and predictable economic performance under uncertainty.

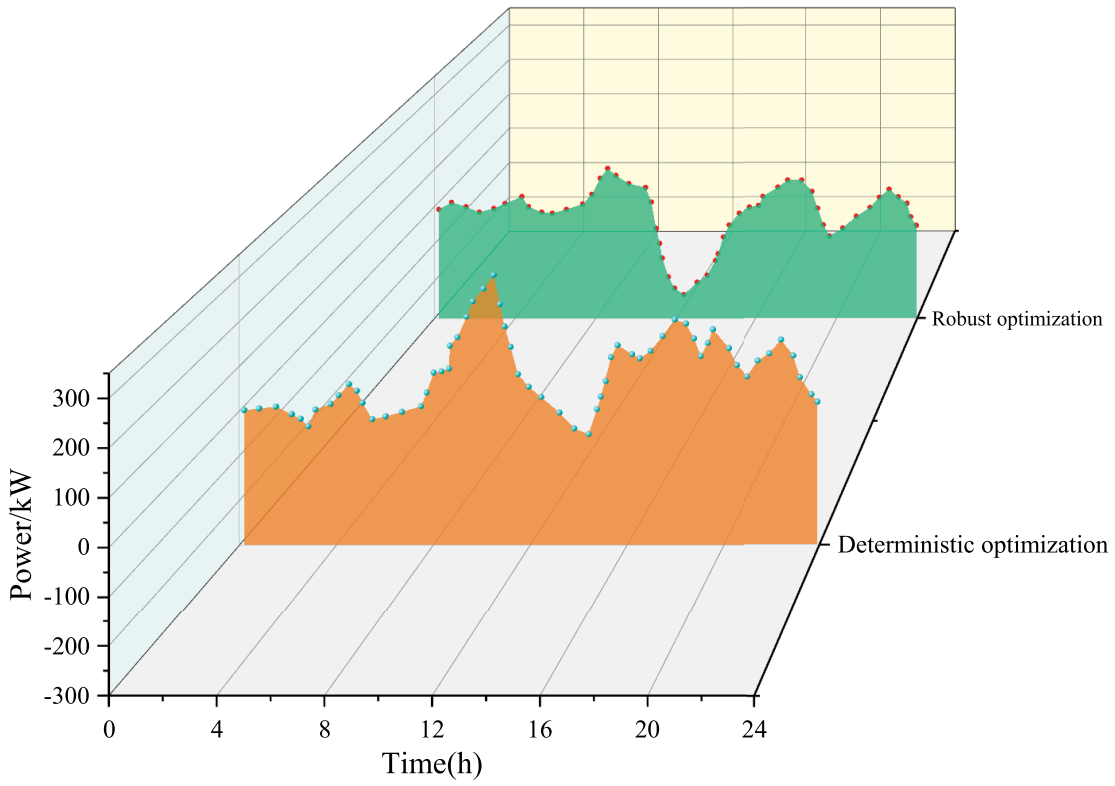

Figure 9: Real-time market imbalance.

Furthermore, the average load loss probability (LPSP) across all feasible scenarios for the robust model was maintained below 0.8%, with the 95th percentile value not exceeding 2.1%. In contrast, the deterministic model, while feasible in some scenarios, exhibited an average LPSP of over 4.5% in its feasible cases, with frequent spikes above 10%. These intermediate metrics—cost stability and supply reliability—collectively prove that the proposed framework not only avoids infeasibility but also ensures consistently high-quality and economically stable operation across a wide range of adverse conditions, thereby enhancing the practical applicability of the strategy.

Comparative analysis of optimization results across different scenarios in Table 3 highlights the trade-offs between robust and deterministic optimization methods. While robust optimization incurs higher daily operating costs, it significantly reduces the market imbalance caused by load and photovoltaic volatility. Fig. 8 illustrates this disparity, where positive values denote excess power purchases and negative values indicate excess power sales by microgrid operators. By selecting a non-stereotypical day as a case study, it becomes evident that the robust optimization schedule results in fewer real-time market purchases compared to the deterministic plan. This reduced market engagement ultimately leads to lower overall operational costs, showcasing the model's ability to balance economic efficiency with resilience in uncertain environments. The findings underscore the importance of integrating robust optimization in scenarios with high renewable penetration, supporting the strategic integration of renewable energy and enhancing the adaptability of energy systems.

As shown in Table 3, the robust optimization approach demonstrates significant resilience by avoiding infeasible scenarios, thereby confirming its robustness against future source-load fluctuations. This characteristic is particularly critical in high-renewable penetration scenarios, where traditional deterministic models often fail to manage the volatility of photovoltaic (PV) outputs and load demands effectively. The robust optimization framework inherently accounts for uncertainties, allowing it to handle the complexities associated with high-penetration renewable energy sources without requiring substantial capital investments. This adaptability ensures that microgrid operators and user-side aggregators can navigate adverse conditions with minimal additional adjustment costs, aligning with the strategic objectives of efficient and sustainable energy management.

A comparative analysis of optimization results across different scenarios, as detailed in Table 3, highlights the trade-offs between robust and deterministic optimization methods. While robust optimization incurs higher daily operating costs, it significantly mitigates market imbalances caused by load and PV volatility. This is illustrated in Fig. 9, where positive values denote excess power purchases and negative values indicate excess power sales by microgrid operators. By examining a non-stereotypical day as a case study, it becomes evident that the robust optimization schedule results in fewer real-time market purchases compared to the deterministic plan. This reduced market engagement ultimately leads to lower overall operational costs, demonstrating the model's ability to balance economic efficiency with resilience in uncertain environments.

The findings underscore the importance of integrating robust optimization in scenarios with high renewable penetration. This approach not only supports the strategic integration of renewable energy but also enhances the adaptability of energy systems, ensuring reliable and economically efficient operations.

3.5 Scalability and Computational Complexity Analysis

While the case study validates the model's effectiveness for a community-scale microgrid, its scalability to larger systems is a critical consideration. The computational complexity of the proposed dual-stage framework primarily stems from the C&CG algorithm in the second stage. The number of binary variables in the master problem is proportional to the scheduling horizon (T = 24 h in this case) and the number of key operational units (e.g., microturbine, storage). The solution time is thus largely dependent on the number of iterations required for convergence, which was shown to be manageable (≈12) for the present scale.

For larger-scale microgrids or multi-microgrid clusters, the complexity would increase polynomially with the number of decision variables and entities (e.g., multiple user aggregators). However, the decomposition nature of the C&CG algorithm makes it amenable to parallel computing techniques, which could be explored in future work to handle larger problems. Furthermore, for near-real-time applications, model predictive control (MPC) could be employed, using the proposed strategy as a backbone for shorter, rolling horizons to reduce computational burden. The solution time of under 5 min reported above confirms the feasibility for day-ahead scheduling, and further optimization of the code could enhance its suitability for larger systems.

4 Conclusion

This article presents a dual-stage game theory-robust optimization-price coupling control (GT-RO-PCC) paradigm to address operational challenges in community-integrated energy microgrids (CIEMs). The paradigm combines strategic interaction mechanisms with uncertainty-aware energy management, establishing a tripartite governance structure. The first stage uses a Stackelberg game-theoretic model for day-ahead electricity/heat pricing strategies, while the second stage constructs a two-stage stochastic robust optimization model to handle uncertainties in wind power and demand predictions. Empirical results show significant improvements in operational cost reduction, wind/PV accommodation rates, energy storage revenue, and carbon reduction. Theoretical contributions include the integration of non-cooperative game theory with distributionally robust optimization and the development of a hierarchical decision protocol.

1. The research introduces a novel dual-stage game theory—robust optimization—price coupling control (GT-RO-PCC) paradigm. This framework synergizes non-cooperative game theory with distributionally robust optimization, establishing a tripartite governance structure among microgrid operators, user-side aggregators, and shared energy storage providers. It advances uncertainty-robust energy management, offering systematic solutions for high-renewable penetration in community-integrated energy microgrids (CIEMs) and supporting China's dual-carbon objectives.
2. The paradigm demonstrates significant cost reduction. Empirical validation shows a daily operational cost reduction of ¥4965.00 (−13.2% vs. baseline). This is achieved through a Stackelberg game-theoretic model that optimizes day-ahead electricity/heat pricing strategies, incorporating flexible load management modeling with carbon emission trading mechanisms.
3. The study achieves high wind/PV accommodation rates of 98.76%/98.91%. The two-stage stochastic robust optimization model addresses Weibull-distributed wind power uncertainty and demand prediction errors, ensuring supply reliability while minimizing operational costs. This model effectively integrates distributed renewable energy sources, enhancing the microgrid's ability to accommodate renewable energy.
4. The research introduces an electricity-carbon coupling mechanism, achieving a 96.95% carbon reduction (1673 kg CO_2/day). By embedding carbon emission trading into the Stackelberg game and linking renewable curtailment penalties to operational costs, the model incentivizes low-carbon behaviors across stakeholders, contributing to the sustainable development goals of the energy system.

5. The paradigm enhances supply resilience to 98.6% under Monte Carlo-simulated extreme scenarios. The robust optimization framework ensures supply reliability under worst-case scenarios while maintaining computational tractability through distributionally robust decision rules. This makes the system more robust and adaptable to uncertainties and risks.

This study's proposed GT-RO-PCC paradigm, while effective, has limitations. The model's assumptions, such as wind speed following a Weibull distribution and load forecasting errors within 3σ confidence intervals, may not fully capture real-world complexities. Additionally, the two-stage optimization model, though robust, has room for computational efficiency improvements. Future research could enhance the model's adaptability by incorporating more flexible uncertainty modeling and advanced forecasting techniques. Furthermore, while the solution time for the community-scale case was acceptable for day-ahead scheduling (approximately 5 min), computational complexity may become a challenge for significantly larger systems with more entities and longer planning horizons. Future research will focus on developing more efficient heuristic algorithms or leveraging distributed computing frameworks to enhance scalability for real-time operation in large-scale networked microgrids.

Acknowledgement: The authors acknowledge China University of Mining and Technology and the Automation College of Huaiyin Institute of Technology for providing the academic environment and support for this research. Thanks are extended to all members of the community microgrid project involved in this study for their assistance in data collection and model validation.

Funding Statement: The authors received no specific funding.

Author Contributions: Siying Li: Methodology, Software, Validation, Formal Analysis, Investigation, Data Curation, Original Draft. Xinyu Feng: Conceptualization, Methodology, Software, Validation, Data Analysis, Original Draft. Xin Ma: Software, Validation, Data Curation, Visualization. Hui Huang: Resources, Data Curation, Supervision. Zhipeng Wang: Conceptualization, Resources, Review & Editing. Baolian Liu and Zujun Ding: Resources, Review & Editing. Weihong Ding: Supervision, Project Administration. Xiaolong Huang: Supervision, Project Administration, Review & Editing. Jie Ji: Conceptualization, Methodology, Resources, Review & Editing, Supervision, Project Administration. All authors reviewed and approved the final version of the manuscript.

Availability of Data and Materials: The numerical data supporting the findings of this study are available from the corresponding author upon reasonable request. The parameters of the Community-Integrated Energy Microgrid (CIEM) system, load data, and renewable energy generation data used in this research are included in the main text and Appendix. To ensure reproducibility, detailed formulations and key parameters of the optimization models are provided in the "Methodology" section and Table A1 in the Appendix.

Ethics Approval: This study did not involve human participants, animal experiments, or personal sensitive data. All analyses were based on anonymized operational data from community microgrids, which contain no personally identifiable information. Therefore, ethical approval was not required for this research.

Conflicts of Interest: The authors declare no conflicts of interest.

Appendix A

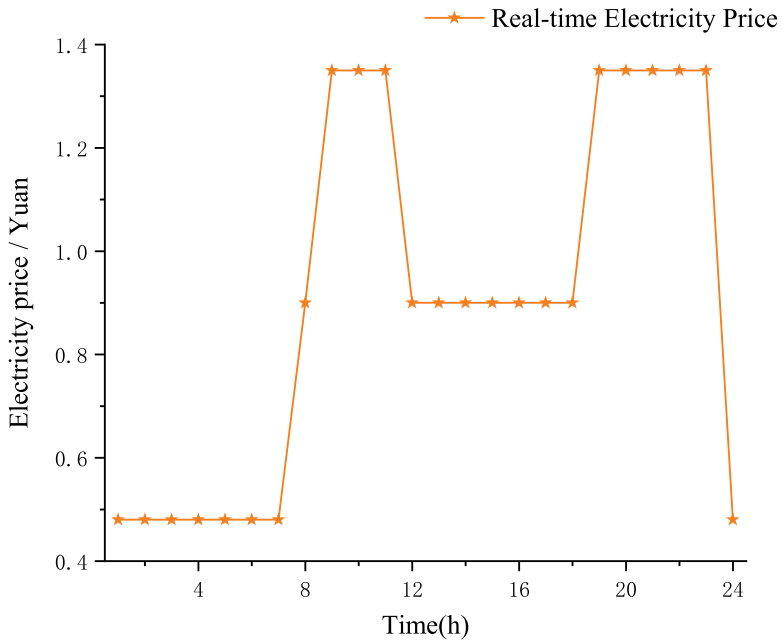

Figure A1: Real-time electricity price.

Table A1: Table of the other parameters of the model.

Object	Parameter	Value
User Aggregator	a	−0.04
	b	4
	c	0
	η_{h}^{l}	0.7
	N	0.3
	β	0.2
	$\Delta Q_{\max}^{l,\mathrm{h}}$	15 kW
	$Q_{\max}^{u,\mathrm{h}}$	60 kW
Shared energy storage system	E_{min}^{ESS}	280 kWh
	E_{max}^{ESS}	1200 kWh
	$P_{\max}^{\mathrm{ESS,c}}$	50 kW
	$P_{\max}^{\mathrm{ESS,d}}$	50 kW
	SOC_0	0.5
	η_{c}^{ESS}	0.96
	η_{d}^{ESS}	0.96

References

1. Us Salam I, Yousif M, Numan M, Billah M. Addressing the challenge of climate change: the role of microgrids in fostering a sustainable future—a comprehensive review. Renew Energy Focus. 2024;48:100538. doi:10.1016/j.ref.2024.100538.
2. Mbasso WF, Harrison A, Jangir P, Dagal I, Khishe M, Smerat A, et al. Reliability-conscious power flow optimization in hybrid renewable microgrids: a case study in Sub-Saharan Africa using Gauss-Seidel and metaheuristic techniques. Int J Electr Power Energy Syst. 2025;173:111350. doi:10.1016/j.ijepes.2025.111350.
3. Chen L, Gao L, Xing S, Chen Z, Wang W. Zero-carbon microgrid: real-world cases, trends, challenges, and future research prospects. Renew Sustain Energy Rev. 2024;203:114720. doi:10.1016/j.rser.2024.114720.
4. Ahmed I, Rehan M, Basit A, Ahmad H, Ahmed W, Ullah N, et al. Review on microgrids design and monitoring approaches for sustainable green energy networks. Sci Rep. 2023;13(1):21663. doi:10.1038/s41598-023-48985-7.
5. Onteru RR, Sandeep V. An intelligent model for efficient load forecasting and sustainable energy management in sustainable microgrids. Discov Sustain. 2024;5(1):170. doi:10.1007/s43621-024-00356-6.
6. Shen X, Li X, Yuan J, Jin Y. A hydrogen-based zero-carbon microgrid demonstration in renewable-rich remote areas: system design and economic feasibility. Appl Energy. 2022;326:120039. doi:10.1016/j.apenergy.2022.120039.
7. Mousa HHH, Mahmoud K, Lehtonen M. A comprehensive review on recent developments of hosting capacity estimation and optimization for active distribution networks. IEEE Access. 2024;12:18545–93. doi:10.1109/ACCESS.2024.3359431.
8. Habib S. Robust load and energy management in smart grids with prosumer-integrated distributed energy resources. J Clean Prod. 2025;496:145138. doi:10.1016/j.jclepro.2025.145138.
9. Chaganti KC. A scalable, lightweight AI-driven security framework for IoT ecosystems: optimization and game theory approaches. IEEE Access. 2025;13:72235–47. doi:10.1109/ACCESS.2025.3558623.
10. Liu ZF, Zhao SX, Luo XF, Huang YH, Gu RZ, Li JX, et al. Two-layer energy dispatching and collaborative optimization of regional integrated energy system considering stakeholders game and flexible load management. Appl Energy. 2025;379:124918. doi:10.1016/j.apenergy.2024.124918.
11. Mojumder MRH, Hasanuzzaman M, Cuce E. Prospects and challenges of renewable energy-based microgrid system in Bangladesh: a comprehensive review. Clean Technol Environ Policy. 2022;24(7):1987–2009. doi:10.1007/s10098-022-02301-5.
12. Akbari S, Camarinha-Matos LM, Martins J. Analyzing value-sharing methods in energy communities with coalitional game theory. In: Technological innovation for human-centric systems. Cham, Switzerland: Springer Nature; 2024. p. 43–60. doi:10.1007/978-3-031-63851-0_3.
13. Alamir N, Kamel S, Megahed TF, Hori M, Abdelkader SM. A multi-layer techno-economic-environmental energy management optimization in cooperative multi-microgrids with demand response program and uncertainties consideration. Sci Rep. 2024;14(1):23418. doi:10.1038/s41598-024-72706-3.
14. Karaki A, Al-Fagih L. Evolutionary game theory as a catalyst in smart grids: from theoretical insights to practical strategies. IEEE Access. 2024;12:186926–40. doi:10.1109/ACCESS.2024.3436935.
15. Malik S. Peer-to-peer energy trading in microgrids: a game-theoretic approach [dissertation]. Galway, Republic of Ireland: University of Galway; 2024.
16. Wang Z, Hou H, Zhao B, Zhang L, Shi Y, Xie C. Risk-averse stochastic capacity planning and P2P trading collaborative optimization for multi-energy microgrids considering carbon emission limitations: an asymmetric Nash bargaining approach. Appl Energy. 2024;357:122505. doi:10.1016/j.apenergy.2023.122505.
17. Wang G, Zhou Y, Lin Z, Zhu S, Qiu R, Chen Y, et al. Robust energy management through aggregation of flexible resources in multi-home micro energy hub. Appl Energy. 2024;357:122471. doi:10.1016/j.apenergy.2023.122471.
18. Zhou Y, Zhai Q, Wu L. Optimal operation of regional microgrids with renewable and energy storage: solution robustness and nonanticipativity against uncertainties. IEEE Trans Smart Grid. 2022;13(6):4218–30. doi:10.1109/TSG.2022.3185231.
19. Li H, Li X, Jin J, Yao H, Jiao Z, Liu J. μ-Synthesis robust coordinated control of variable speed wind power generators and electric vehicles to regulate frequency. Energy Rep. 2023;9:584–95. doi:10.1016/j.egyr.2023.04.123.

20. Li X, Liu Y, Guo L, Li X, Wang C. Data-driven based uncertainty set modeling method for microgrid robust optimization with correlated wind power. CSEE J Power Energy Syst. 2023;9(2):420–32. doi:10.17775/CSEEJPES.2021.06330.
21. Omri M, Jooshaki M, Abbaspour A, Fotuhi-Firuzabad M. Modeling microgrids for analytical distribution system reliability evaluation. IEEE Trans Power Syst. 2024;39(5):6319–31. doi:10.1109/TPWRS.2024.3354299.
22. Hedayatnia A, Ghafourian J, Sepehrzad R, Al-Durrad A, Anvari-Moghaddam A. Two-stage data-driven optimal energy management and dynamic real-time operation in networked microgrid based on a deep reinforcement learning approach. Int J Electr Power Energy Syst. 2024;160:110142. doi:10.1016/j.ijepes.2024.110142.
23. Meng Q, Hussain S, Luo F, Wang Z, Jin X. An online reinforcement learning-based energy management strategy for microgrids with centralized control. IEEE Trans Ind Appl. 2025;61(1):1501–10. doi:10.1109/TIA.2024.3430264.
24. Aldahmashi J, Ma X. Real-time energy management in smart homes through deep reinforcement learning. IEEE Access. 2024;12:43155–72. doi:10.1109/ACCESS.2024.3375771.
25. Goh HH, Huang Y, Lim CS, Zhang D, Liu H, Dai W, et al. An assessment of multistage reward function design for deep reinforcement learning-based microgrid energy management. IEEE Trans Smart Grid. 2022;13(6):4300–11. doi:10.1109/TSG.2022.3179567.
26. dos Santos FS, do Nascimento KKF, da Silva Jale J, Xavier SFA, Ferreira TAE. Brazilian wind energy generation potential using mixtures of Weibull distributions. Renew Sustain Energy Rev. 2024;189:113990. doi:10.1016/j.rser.2023.113990.
27. Zheng L, Li H, Ran L, Gao L, Xia D. Distributed primal–dual algorithms for stochastic generalized Nash equilibrium seeking under full and partial-decision information. IEEE Trans Control Netw Syst. 2023;10(2):718–30. doi:10.1109/TCNS.2022.3204813.
28. Gautam M. Evolutionary game dynamics between distributed energy resources and microgrid operator: balancing act for power factor improvement. Electronics. 2024;13(2):248. doi:10.3390/electronics13020248.
29. Ayop R, Isa NM, Tan CW. Components sizing of photovoltaic stand-alone system based on loss of power supply probability. Renew Sustain Energy Rev. 2018;81:2731–43. doi:10.1016/j.rser.2017.06.079.
30. Gawusu S, Ahmed A. Analyzing variability in urban energy poverty: a stochastic modeling and Monte Carlo simulation approach. Energy. 2024;304:132194. doi:10.1016/j.energy.2024.132194.